CONTROL CHARACTERISTICS OF AN AUTOMATIC PILOT FOR AIRCRAFT

by

LtCdr. Frank M. Ralston, U.S.N.
Comdr. Hamilton C. Hauck, U.S.N.
Comdr. George A. Whiteside, U.S.N.

(Inter-Departmental)

MASSACHUSETTS INSTITUTE OF TECHNOLOGY

Cambridge 39, Mass.

OFFICE OF C. S. Draper

Memorandum to: Captain W. H. Buracker

From: Dr. C. S. Draper

Date: September 4, 1946

Subject: Thesis Work of Lt. Comdr. F.M. Ralston
Comdr. H. O. Hauck
Comdr. G. A. Whitesides

The Officers listed above have recently submitted a Master's Thesis done under my supervision entitled:

"Control Characteristics of An Automatic Pilot For Aircraft."

Good technique and a sound approach produced a good experimental determination of the operating characteristics to be expected from the automatic pilot studied in the thesis work. The officers concerned should receive particular credit for intelligent application of the principles taught during their year of graduate work. Their workmanlike attack in designing, building, and using a complicated laboratory test installation in the short time available represents an excellent job.

/s/ C. S. Draper
Chairman of Graduate Committee
Department of Aeronautical Engineering

CSD:pm

(Inter-Departmental)

MASSACHUSETTS INSTITUTE OF TECHNOLOGY

Cambridge 39, Mass.

OFFICE OF C. S. Draper

Memorandum to: Captain W. H. Buracker

From: Dr. C. S. Draper

Date: September 4, 1946

Subject: Thesis Work of Lt. Comdr. F.M Ralston
Comdr. H. O. Hauck
Comdr. G. A. Whiteside

The Officers listed above have recently submitted a Master's Thesis done under my supervision entitled:

"Control Characteristics of An Automatic Pilot For Aircraft."

Good technique and a sound approach produced a good experimental determination of the operating characteristics to be expected from the automatic pilot studied in the thesis work. The officers concerned should receive particular credit for intelligent application of the principles taught during their year of graduate work. Their workmanlike attack in designing, building, and using a complicated laboratory test installation in the short time available represents an excellent job.

/s/ C. S. Draper
Chairman of Graduate Committee
Department of Aeronautical Engineering

CSD:pm

CONTROL CHARACTERISTICS OF AN AUTOMATIC PILOT FOR AIRCRAFT

by

Lt. Comdr. Frank M. Ralston, U. S. Navy
B.S., U. S. Naval Academy, Annapolis, Maryland
1939

Comdr. Hamilton O. Hauck, U. S. Navy
B.S., U. S. Naval Academy, Annapolis, Maryland
1938

Comdr. George A. Whiteside, U. S. Navy
B.S., U. S. Naval Academy, Annapolis, Maryland
1938

Submitted in Partial Fulfillment of the Requirements

for the Degree of

Master of Science (Aeronautical Engineering)

from the

Massachusetts Institute of Technology

1946

Signatures of Authors _____

_____

_____

Department of Aeronautical Engineering, August 24, 1946.

Signature of Professor in Charge
of Research _____

Signature of Chairman of Department
Committee on Graduate Students _____

August 24, 1946.

Professor Joseph S. Newell,
Secretary of the Faculty,
Massachusetts Institute of Technology,
Cambridge, Massachusetts.

Dear Sir:

We hereby submit the enclosed thesis entitled, "Control Characteristics of an Automatic Pilot for Aircraft", in partial fulfillment of the requirements for the degree of Master of Science (Aeronautical Engineering) from the Massachusetts Institute of Technology.

Respectfully yours,

Frank M. Ralston

Hamilton O. Hauck

George A. Whiteside

ACKNOWLEDGMENT

The authors wish to take this opportunity to express their appreciation for the valuable suggestions and assistance rendered by Professor R. C. Seamans, Jr. and Mr. Howard Carson.

To Mr. Frank Wilkins we feel indebted for his assistance in setting up and operating the recording equipment.

Grateful acknowledgment is given to the Aero Division of the Minneapolis-Honeywell Company for providing supplementary data about the automatic pilot.

TABLE OF CONTENTS

ILLUSTRATIONS

TABLES

SYMBOLS

A - Aeronautical Engineering.

g - Standard acceleration of gravity = 32.174 ft/sec^2 or 386 in/sec^2.

ρ_o - Standard density of dry air at sea level = .002378 lb ft^{-4} sec^2.

ρ - Density of air at altitude.

S - Area.

S_w - Area of wing.

S_t - Area of tail.

V - True airspeed.

q - Dynamic pressure = $1/2 \rho V^2$.

α - Angle of attack.

C_{H_δ} - Hinge moment coefficient due to elevator angle setting.

δ - Elevator angle.

M_H, H - Hinge moment.

$\frac{\partial M_H}{\partial \delta_e}$ - Torsional elasticity of elevator.

K - Elastic coefficient of spring (pounds per inch).

I - Moment of inertia.

ω_n - Natural frequency of oscillation of second order system.

C - Viscous damping coefficient.

c - Chord length - Appropriate subscripts added to specify surface.

S - Distance travelled by airplane, measured in 1/2 wing chords.

SYMBOLS
(Cont'd)

B - Servomechanisms.

θ_i - Angular motion of flight gyro wiper - measured in degrees.

θ_m - Angular motion of servomotor cable drum - measured in degrees.

θ_o - Angular motion of elevator - measured in degrees.

θ_{m_i} - Angular motion of servomotor cable drum referred to the flight gyro wiper. Under conditions of perfect motor response, $\theta_m = 2\theta_i$. Hence $\theta_{mi} = \frac{\theta_m}{2}$.

θ_{o_i} - Angular motion of elevator referred to the flight gyro wiper. Under conditions of perfect motor response and no cable stretching, $\theta_o = .468\theta_i$. Hence $\theta_{o_i} = \frac{\theta_o}{.468} = 2.135\ \theta_o$.

ε_m - Angular error of cable drum from flight gyro wiper, $E_m = \theta_i - \theta_{mi}$ where quantities are vectors.

- Transfer function, = $\frac{\text{Output of unit (vector)}}{\text{Input to unit (vector)}}$

γ - Damping ratio = $\frac{\text{system damping coefficient}}{\text{system critical damping coefficient}}$

SUMMARY

The purpose of this investigation was to determine the control characteristics of an automatic pilot for aircraft. The automatic pilot used was the Minneapolis-Honeywell type C-1A autopilot. The load applied to the autopilot consisted of inertia, elastic restraint, and coulomb friction, all embodied in a test apparatus. For the purpose of this investigation, the test apparatus was made to simulate the elevators of a Douglas A-26 attack bomber. Three different values of indicated airspeed were simulated, 200, 250, and 350 miles per hour. The conditions assumed were that the airplane was in normal flight and was not allowed to respond to the elevator action.

As a result of this investigation the characteristics of this autopilot were determined. Increasing the indicated airspeed increases the torque output of the servomotor and decreases the elevator shaft rotation for a given input signal. The resonant frequency of the system increases slightly with an increase of indicated airspeed. The effective damping of the system decreases with an increase of airspeed. The effect of the control cable is to decrease the magnitude of the elevator shaft rotation, this effect increasing as indicated airspeed increases. The automatic pilot is stable throughout the range of airspeeds investigated and is a satisfactory servomechanism.

This investigation was conducted at the Massachusetts Institute of Technology Aeronautical Engineering Laboratory from June to August, 1946.

INTRODUCTION

Although automatic pilots for aircraft have been in use for many years, comparatively little data is available concerning their actual performance as servomechanisms under the aerodynamic load conditions encountered in flight. The purpose of this investigation was to determine the performance of a typical automatic pilot, and its components, under artificial loads calculated to duplicate those imposed upon the mechanism under various flight conditions. It is emphasized that this investigation includes only the automatic pilot, the control cables, and the control surface - considered as a servomechanism. The response of the airplane to the resultant control surface movement has not been included and the assumption has been made that the airplane continues essentially unchanged along its flight path at the prescribed airspeed.

The automatic pilot employed in this study was the Minneapolis-Honeywell, Type C1A. This pilot was selected because it appears typical of the designs to be encountered in the future and because several concurrent investigations, using this autopilot in actual aircraft, are being conducted.

The test assembly for the investigation was constructed to duplicate the elevator control system of a medium bomber type aircraft. Since the necessary structural and aerodynamic data for the A-36 Attack Bomber were available, the

artificial loads were computed to simulate closely those which are encountered by automatic pilot installations in that aircraft. Aerodynamic viscous damping forces resulting from elevator motion were computed but, due to time limitations, no viscous damper was installed on the test assembly. Computations showed the relative magnitudes of these forces to be small. However, provision was made for incorporating this feature in future investigations by machining threads at the end of the elevator shaft for the viscous damper fitting, and by including a chart of the viscous damping coefficients versus true airspeed.

It was anticipated that the cable from the servo motor to the elevator horn would have considerable effect upon the performance of the system. Therefore, the length of cable and the size of the elevator horn were made to duplicate the corresponding dimensions of the A-26.

The more important data required for this investigation were the magnitude and phase relations of the elevator angular position, the angular position of the servomotor cable drum, and the torque delivered at the load, to the input signal generated by sinusoidal movement of the flight gyro potentiometer wiper. The amplitude of this sinusoidal wiper motion was fixed at 7 1/2 degrees either side of mid-position and the frequency of motion varied from .05 to 4 cycles per second (approx.).

The transfer locus system of analysis is employed herein to evaluate the performance of the system as a whole, and to evaluate the contributions of the system components. In submitting this report, the authors pre-suppose a familiarity on the part of the reader with transfer loci studies, the Nyquist diagram and stability criteria, and transfer functions employing the LaPlace transform. To augment the transfer loci plotted herein, plots of the amplitude and phase response of various system components have been made on Cartesian coordinates.

This investigation was conducted in the Instrumentation Laboratory of the Massachusetts Institute of Technology by the authors of this report.

EQUIPMENT AND PROCEDURE

Photographs of the equipment employed in the tests are provided in Figs. 1 and 2. The equipment may be grouped in three major components. Referring to the photographs, group A includes the units of the recording oscillograph which provided timed records of the various performance data. This unit possessed twelve separate data channels, of which six channels were used. Group B includes the necessary units of the Minneapolis-Honeywell C1A automatic pilot for conducting the tests. Only the elevator channel of the automatic pilot was employed. Group C is the test assembly which simulates the elevator control arrangement of an A-26 airplane, and further provides for imposing artificial aerodynamic loads on the system.

In group B, (1) is the sine drive mechanism which moves the wiper (2) of the elevator flight gyro potentiometer (removed from the flight gyro unit for these tests) sinusoidally through an amplitude of 7 1/2 degrees each side of the center of the potentiometer - or a total swing of 15 degrees. The position of this input wiper was recorded by the synchro (3) mounted on the wiper shaft. Its output voltage was applied to the recording oscillograph. The synchro was adjusted to provide zero voltage on the record when the input wiper was in mid-position. The frequency of the input motion was adjusted

by Variac control of the sine drive electric motor, providing a frequency range from .05 to 4 cycles per second.

The servo motor (15) which drives the control cable drum is provided with a potentiometer, the wiper of which is directly connected to the cable drum shaft. The input potentiometer and the motor potentiometer are connected electrically so that with the motor drum position matched to the input wiper position, no error voltage is developed between the wipers. When the cable drum position is not matched with the input, an error voltage is developed between the wipers. This voltage is applied to the amplifier (4) which amplifies the error voltage, discriminates between errors on either side of the matched condition, and energizes the correct relay (5) to drive the servo motor in a direction to erase the error. A sketch of the discriminator circuit is shown in Fig. 6. The electrical system is so arranged that one degree of motion at the input wiper results in two degrees of motion of the cable drum. Under perfectly matched conditions, therefore, the cable drum moves through a total swing of 30 degrees, or a sine amplitude of 15 degrees.

The construction of this automatic pilot is such that the following action of the servo motor is not continuous. The action is better described as a "pecking" action whereby the motor is driven in pulses until the error is erased. During these pulses, the motor brake is off and voltage is applied to the motor terminals. Between pulses, no voltage is applied to

the motor terminals, and the solenoid-operated brake prevents rotation of the cable drum. If the error exceeds a set amount, pecking action ceases and the proper relay is held down until the error has decreased to the pecking action range. The frequency of pecking is determined by a time-delay network incorporated in the discriminator circuit.

A synchro, like that installed on the input potentiometer, was attached to the cable drum shaft to provide a means of recording the servo motor response.

In group C, the units were made to duplicate as closely as possible the more important dimensions of the A-26 elevator assembly. The cable (6) distance from servo motor to elevator hinge (8) and the dimensions of the elevator horn (7) are the same as those in the A-26. Inertia weights (9) were added to increase the inertia of the system to that of the A-26 elevator about its hinge axis. (See "Sample Calculations"). Coulomb friction of the A-26 elevator control system was duplicated by adjustment of the prony brake (10) bearing against the friction disc (11). A viscous damper fitting (12) was provided at the end of the elevator shaft. During the tests, no viscous damper was installed because of shortage of time, and because the magnitudes, as developed in "Sample Calculations" and shown in Fig. 3, were deemed negligible. It was found that coulomb friction alone was sufficiently large to damp out oscillations rapidly. However, the data of Fig. 3 has

been included so that further tests with this equipment may provide the viscous damping feature.

The elevator torsional elasticity was simulated by springs (13) installed at the ends of torque arms (14) mounted on the elevator shaft. The springs were fixed to the test table at their lower ends. The required elastic coefficients of the springs were determined as shown in "Sample Calculations". A plot of these coefficients is given in Fig. 4, which was derived from the torsional elasticity computations in "Sample Calculations" - a plot of which is shown in Fig. 5.

A synchro (16) was fitted to the elevator shaft to provide a record of the elevator position versus time. Strain gauges (17) were installed on the elevator horn to provide a record of the torque on the elevator versus time.

In order to obtain sufficient data to plot the frequency response of the system and, subsequently, to analyze the performance of system components, the following data items, arranged in their order of appearance (vertically downward) on the record (Fig. 8), were obtained:

(a) Angular position of flight gyro potentiometer.

(b) Angular position of servo motor cable drum.

(c) Motor relay closure, or times of application of voltage to the motor - and direction of applied voltage.

(d) Angular position of elevator.

(e) Error voltage, measured at the grid of the amplifier (7F7) tube.

(f) Torque, measured at the elevator shaft - calibrated in lb. ft. as shown in Fig. 7.

Tests were made with aerodynamic loads corresponding to 200, 250 and 350 miles per hour, indicated. During each of these tests, the input sinusoidal frequency was varied from approximately .05 to 4 cycles per second and simultaneous values of the data listed above were recorded by the oscillograph. Upon completion of the tests, the oscillograph records were developed, printed, and data was taken from them for entry on the enclosed data sheets.

RESULTS AND DISCUSSION

The results obtained in this investigation are very satisfactory. The virtual absence of "wild" readings is directly attributable to the excellent performance of the recording oscillograph. For the conduct of experiments or tests where many quantities must be simultaneously recorded, the advantages of this instrument in accuracy, and in saving time and labor, are great.

Results are graphically presented in Figs. 10 through 23 and are tabulated in Tables I through IX. Figs. 10 and 11 are plots of the amplitude and phase response, respectively, of the servomotor (measured at the cable drum) and the elevator, with an airspeed of 200 mph (ind). It is seen that at frequencies below 0.5 cps the amplitude response of the servomotor is practically constant at a value of 0.88. In this same frequency range, the elevator amplitude response is similarly constant but with a value of approximately 0.6. It will be noted from Fig. 11 that the phase lags of the servomotor and the elevator are identical and that this lag increases almost linearly with frequency in the low frequencies. As the frequency is increased, the amplitude response rises gradually to a peak value of 0.965 for the servomotor and 0.708 for the elevator, at a resonant frequency of approximately 1.04 cps. The phase angle continues its gradual rise until the resonant frequency is approached, when it rises sharply, swings rapidly through the

90 degree value, and thereafter increases more rapidly with frequency than it did in the low frequency range. Past resonance, the amplitude responses of both servomotor and elevator drop off sharply and then asymptotically approach zero - with values at the highest recorded frequency (2.9 cps) of .200 and .175 respectively.

Figs. 12 and 13 are the amplitude and phase response curves, for an airspeed of 250 mph (ind). Figs. 14 and 15 are similar curves for an airspeed of 350 mph (ind). These curves have the same general configuration as the curves of Figs. 10 and 11 described above, although the constant amplitude response at low frequencies is no longer present. The 250 mph curves show that the amplitude responses are smaller, throughout the total frequency range, than that for 200 mph, with peak amplitude response for the motor at .950 and for the elevator at .622.

A further decrease in the general amplitude response is apparent when the airspeed is increased to 350 mph. Peak amplitude responses become .893 for the motor and .433 for the elevator. The phase lag decreases slightly with increased airspeed, while the resonant frequencies increase to 1.25 cps at 250 mph and 1.28 cps at 350 mph.

Figs. 16, 17, and 18 combine the information presented in Figs. 10 through 15 and present it in polar form. Fig. 19 shows the transfer loci of the automatic pilot at 200, 250 and 350 mph. These are plots of the transfer functions of

the autopilot, obtained by vectorially dividing the servomotor output by the error between the input wiper and the cable drum.

Figs. 20, 21, and 22 show the magnitudes of torque developed at the elevator hinge at the three airspeeds employed, plotted against frequency. The phase lag of the torques is presented in the same figures.

Fig. 23 is a plot, on Cartesian coordinates, of the effect of cable stretching at each airspeed. The values plotted are the values of the transfer function of the cable at various frequencies.

Fig. 24 is a reproduction of a typical data record obtained by the oscilloscope. The smallest timed line spacing is .01 seconds. Calibration data for the oscilloscope is given in Table X.

A comparison of Figs. 10, 12, 14, 16, 17, and 18 shows that as the load, i.e., the simulated airspeed, is increased, the output angle at the elevator shaft becomes smaller for a given input signal. For a given load the output amplitude is not a constant but varies with the frequency of the input. There is a greater difference in response between any two loads at low frequencies than at high frequencies. This is attributed to the fact that the load consisted of inertia, elastic restraint, and coulomb friction. Changes of load were accomplished by changes of elastic restraint, the inertia and coulomb friction remaining unchanged. At low frequencies the

governing factor of the load is the elastic restraint and at high frequencies the governing factor is the inertia. Therefore, larger changes in the response at low frequencies are to be expected while only minor changes in the response are to be expected at the higher frequencies.

The motor output to signal input ratio is always less than unity at low frequencies. When operating near the minimum error voltage level the peck duration is a function of the amount of error. The amount of torque delivered by the motor is a linear function of the peck duration. Therefore, the torque output is a function of the amount of error. For stiff loads with consequent high torques to be overcome, a greater minimum error is required at low frequencies.

The fact that the motor output to signal input ratio is always less than unity at very low frequencies can be explained by the fact that the autopilot does not have a zero position error. This fact is illustrated in Fig. 19. For a zero position error, the loci would approach the - j w axis asymptotically. A minimum voltage error must exist before the relays can operate. This voltage level exists independently of load and can be considered dead space.

The elevator shaft output to signal input ratio curve is similar in shape to the motor output to signal input ratio curve. The curves would be identical if the motor and elevator shafts were rigidly connected. The difference between the two

curves is then caused by the cable connecting the two shafts. Fig. 23 shows a plot of the transfer locus of the cable. If the motor output to signal input ratio is multiplied by the amplitude ratio from Fig. 23, the elevator shaft output to signal input ratio is obtained.

The amplitude ratio curves, Figs. 10, 12, and 14, show definite resonance effects and a falling off of response at higher frequencies. The resonant frequency increases slightly with increase of load. The average resonant frequency obtained was about 1.2 cycles per second. The resonant effect becomes more marked as the load increases. This indicates that the effective damping is less for larger loads.

Figs. 11, 13, and 15 show the phase response of the motor shaft and elevator shaft outputs. Since there is a zero phase shift occurring in the cable, the motor and elevator shaft output phase angles are the same. These curves show that the resonant frequency increases for an increased load and that the average resonant frequency obtained for the loads used was about 1.2 cycles per second. Other than changing the resonant point slightly, the load appears to have little effect upon the phase response. Increasing the load decreases the phase angle slightly.

The torque applied to the elevator shaft is shown in Fig. 20, 21, and 22. A comparison of these three curves shows that as the load increases the torque applied to the load in-

creases. All curves have a definite resonance effect with the resonant frequency increasing slightly with load. The average resonant frequency was about 1.2 cycles per second. The phase angle of the torque at the load is essentially unchanged by changes of load. In all cases the phase of the torque leads the phase of the elevator shaft angle.

Fig. 23 shows a plot of the transfer function of the cable for the three different loads used. The cable used for this investigation was a 3/32 inch flexible wire cable with an initial tension of about sixty pounds. This corresponded to an ambient temperature of about seventy degrees Fahrenheit. Previous to the investigation for this report, a series of runs were made with a 1/8 inch extra flexible wire cable. From the results of these two series of runs it appears that decreasing the size of the cable, increasing the elasticity of the coupling, also decreases the torque and the output angle at the elevator shaft for a given input. The curves of Fig. 23 were obtained by dividing the output of the cable, elevator shaft rotation, by the input to the cable, motor shaft rotation. The cable effect seems to be a scalar effect since the phase angle remained zero throughout. However, the cable exerted an effect which does not appear as a phase angle. This effect was in causing the elevator output angle to appear distorted from a sinusoidal variation. The oscillation began at the same time that the motor shaft oscillation began, but the maximum amplitude occurred at a later time than the motor shaft maximum amplitude.

The viscous damping coefficients that are applicable to the various airspeeds used are shown in Fig. 3. No viscous damping was intentionally introduced in this test apparatus since the effect was considered almost negligible and because of a shortage of time available for the investigation. Coulomb friction was introduced into the apparatus, however, and was set to give a force of ten pounds in the control cable. This friction caused an effective damping ratio, ζ, to appear.

The natural frequency of the system is 1.6 cycles per second as found from Fig. 19. Figs. 10, 12, and 14 show that the resonant frequencies for the various loads are 1.04, 1.25, and 1.28 cycles per second respectively for the 200, 250, and 350 miles per hour conditions. With this information and Plate 12, Chapter VII, Instrument Analysis (Draper and McKay), the damping ratios can be computed. Using this technique, the damping ratios are 0.54, 0.36, and 0.34 for airspeeds of 200, 250, and 350 miles per hour respectively. This was expected since the same amount of coulomb friction would have less effect on large loads than on small loads. The natural frequency as calculated by this method is again 1.6 cycles per second.

Fig. 19 shows that the system is stable throughout the entire range of airspeeds investigated. Instability would be denoted by enclosure of the $-1 + j\,0$ point within the transfer locus. Referring to this figure, the system shows sufficient stability. The sensitivity of the system could be increased by a factor of 3.86 : 1 before instability would occur for the

range of airspeeds investigated. This increased sensitivity would result in an increasing ratio of elevator shaft rotation to signal input at resonance.

CONCLUSIONS

An analysis of the results of this investigation substantiates the below-stated conclusions of the general control characteristics of the Minneapolis-Honeywell type C-1A automatic pilot:

(1) The "autopilot" is a satisfactory servomechanism with ample stability. The resonant frequencies are sufficiently high that no resonance effect will be encountered during normal flight operations. The use of a series wound D.C. motor controlled by relays with "pecking" action closely approximates a proportional servo and appears to be an excellent design practice in view of the weight saving accomplished.

(2) At low frequencies the response of the servo motor is appreciably affected by the load stiffness. An increase in load stiffness, i.e., indicated airspeed, decreases the amplitude of the response.

(3) At very high frequencies the response is governed principally by the load inertia and is only very slightly affected by the load stiffness. The frequencies of normal application are well below this range.

(4) The torque output of the motor is proportional to the motor matching error for small angles of matching error after "pecking" action starts. When outside this small linear range the torque output is governed by the torque-speed characteristics of the servomotor. Motor torque output is increased by an increase of load stiffness or a decrease of input frequency.

(5) The servo has a "zero dead space" and is not a zero positional error servomechanism. The magnitude of this dead space is a function of the voltage sensitivity of the potentiometer and of the current sensitivity of the relays. The dead space could be reduced by increasing either of these sensitivities.

(6) The elastance of the coupling between the motor and the elevator shaft has a detrimental effect on the overall servomechanism performance. This effect becomes greater as torques become greater or as the load to motor coupling becomes less rigid.

(7) Coulomb friction caused the system to have an effective damping ratio, ζ. The effective damping ratio decreased as the indicated airspeed was increased. The resonant frequency also shifted,

increasing as the indicated airspeed was increased.

(8) The system natural frequency was so governed by the amplifier and motor characteristics that it remained constant at 1.6 cycles per second independently of load stiffness.

RECOMMENDATIONS

The below recommendations are divided into two main groups. Group A is recommendations for improving the control characteristics of the "autopilot", while Group B is recommendations for further investigations.

A - Recommendations for improving the control characteristics.

(1) Increase the sensitivity of the A.C. bridge potentiometers.

(2) Redesign the relays to be more sensitive and to provide larger contact areas.

(3) Incorporate an integral effect for the relays by making the "peck" duration a function of the magnitude of the error and the length of time that the error has existed.

(4) Minimize the elastic effect of the cable by using gears, multiple cables, or putting an A.C. bridge potentiometer on the output shaft.

B - Recommendations for further investigations.

(1) The input signal amplitude should be kept to a maximum value of about 2.0 degrees.

(2) Investigate the no load frequency response of the servo motor.

(3) Determine the torque-speed characteristics of the servo motor.

(4) Make a series of tests using a series of values of elastic coupling between motor and load.

(5) Investigate the control characteristics with the motor potentiometer installed on the elevator shaft.

(6) Incorporate a viscous damper on the elevator shaft.

(7) Investigate the response at frequencies bracketing the natural frequency of the output load.

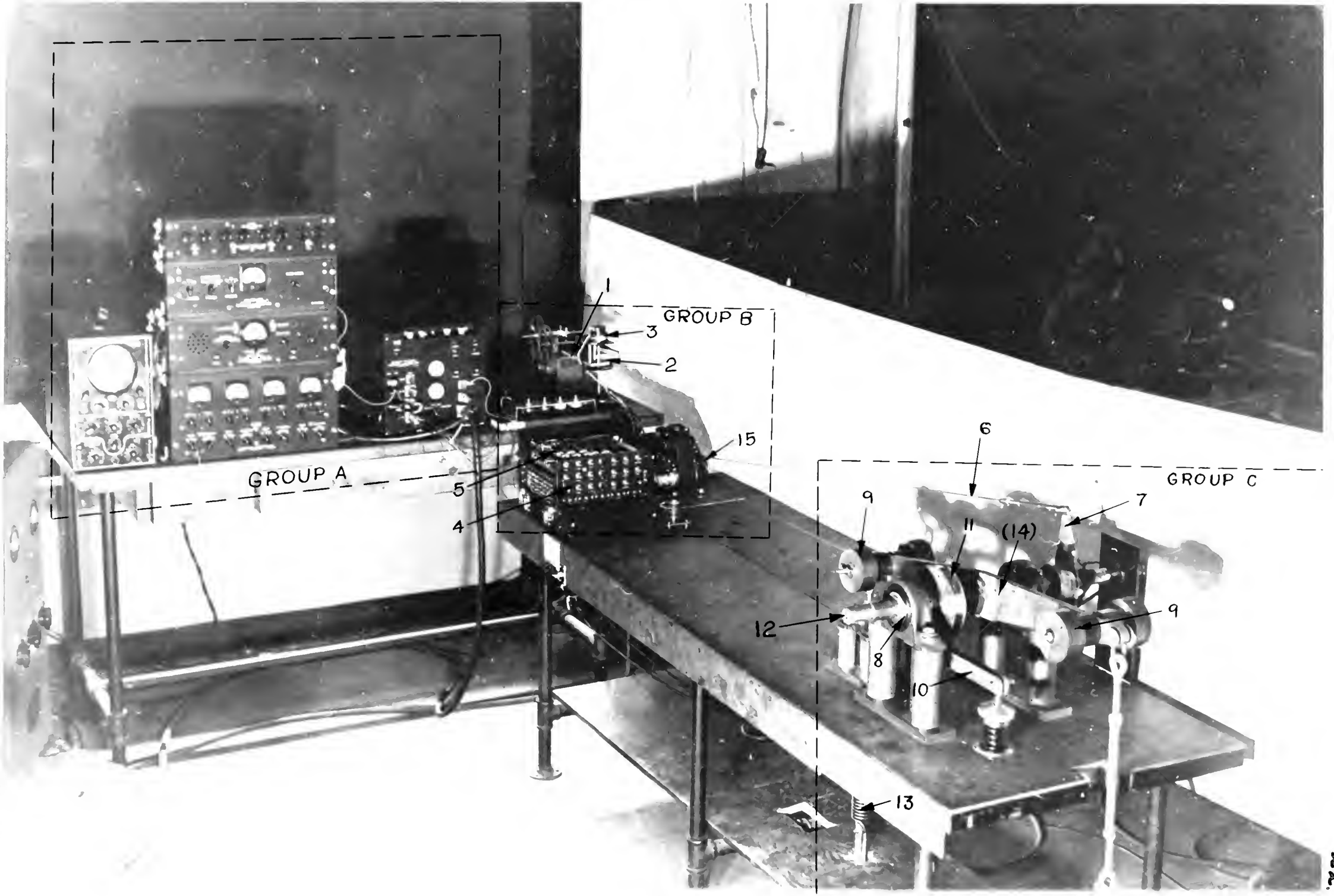
GROUP A
GROUP B
GROUP C
1
2
3
4
5
6
7
9
9
10
11
(14)
12
13
15

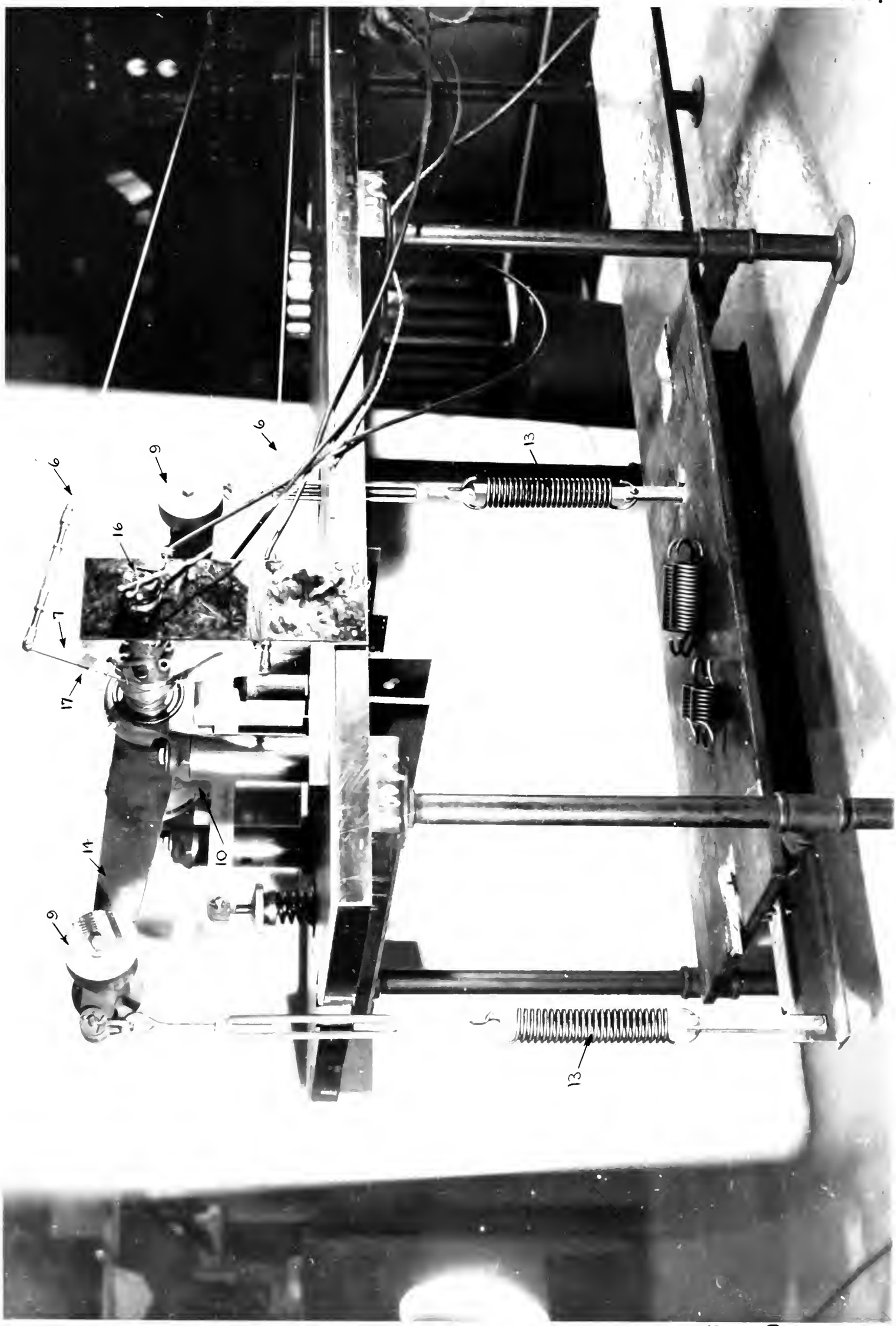

Fig. 2

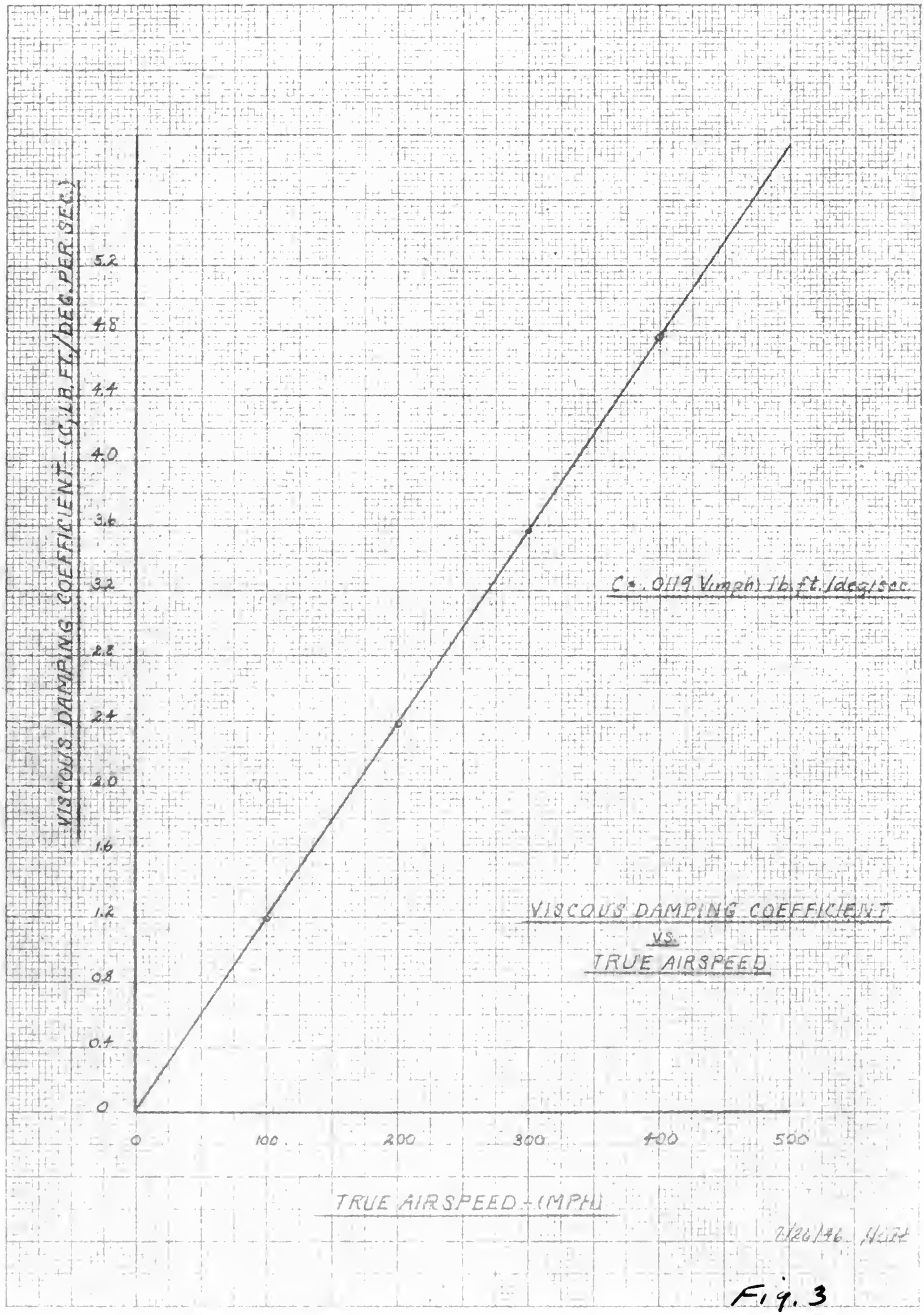
VISCOUS DAMPING COEFFICIENT - (C) LB. FT./DEG. PER SEC.
5.2
4.8
4.4
4.0
3.6
3.2
2.8
2.4
2.0
1.6
1.2
0.8
0.4
0
0
100
200
300
400
500
TRUE AIRSPEED - (MPH)
C = .0119 V (mph) lb. ft. / deg / sec.
VISCOUS DAMPING COEFFICIENT
VS.
TRUE AIRSPEED
2/26/46 H.S.P.

Fig. 3

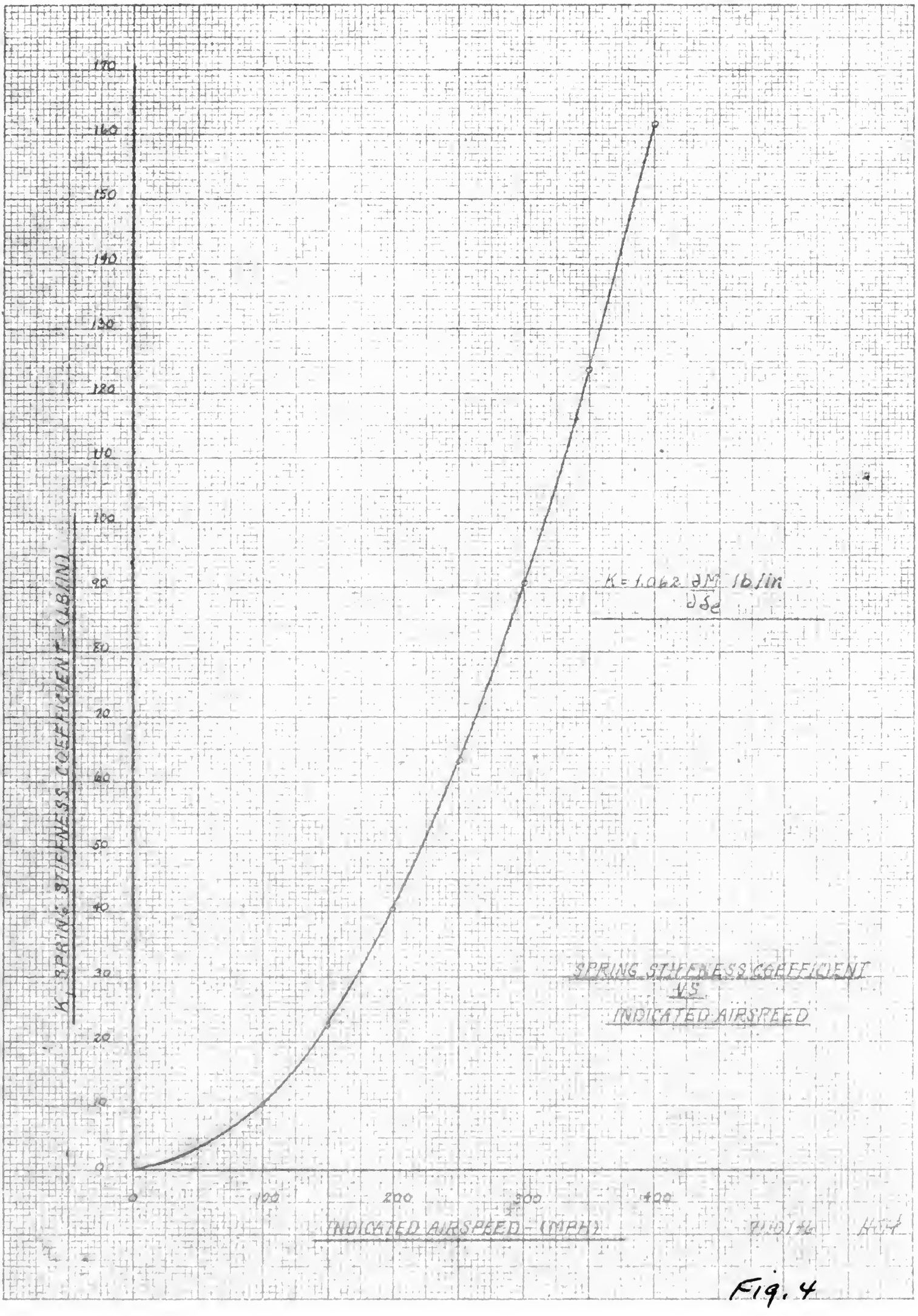
K = 1.062 ∂M/∂δe lb/in
SPRING STIFFNESS COEFFICIENT VS INDICATED AIRSPEED
K - SPRING STIFFNESS COEFFICIENT - (LB/IN)
INDICATED AIRSPEED - (MPH)
0
100
200
300
400
10
20
30
40
50
60
70
80
90
100
110
120
130
140
150
160
170

Fig. 4

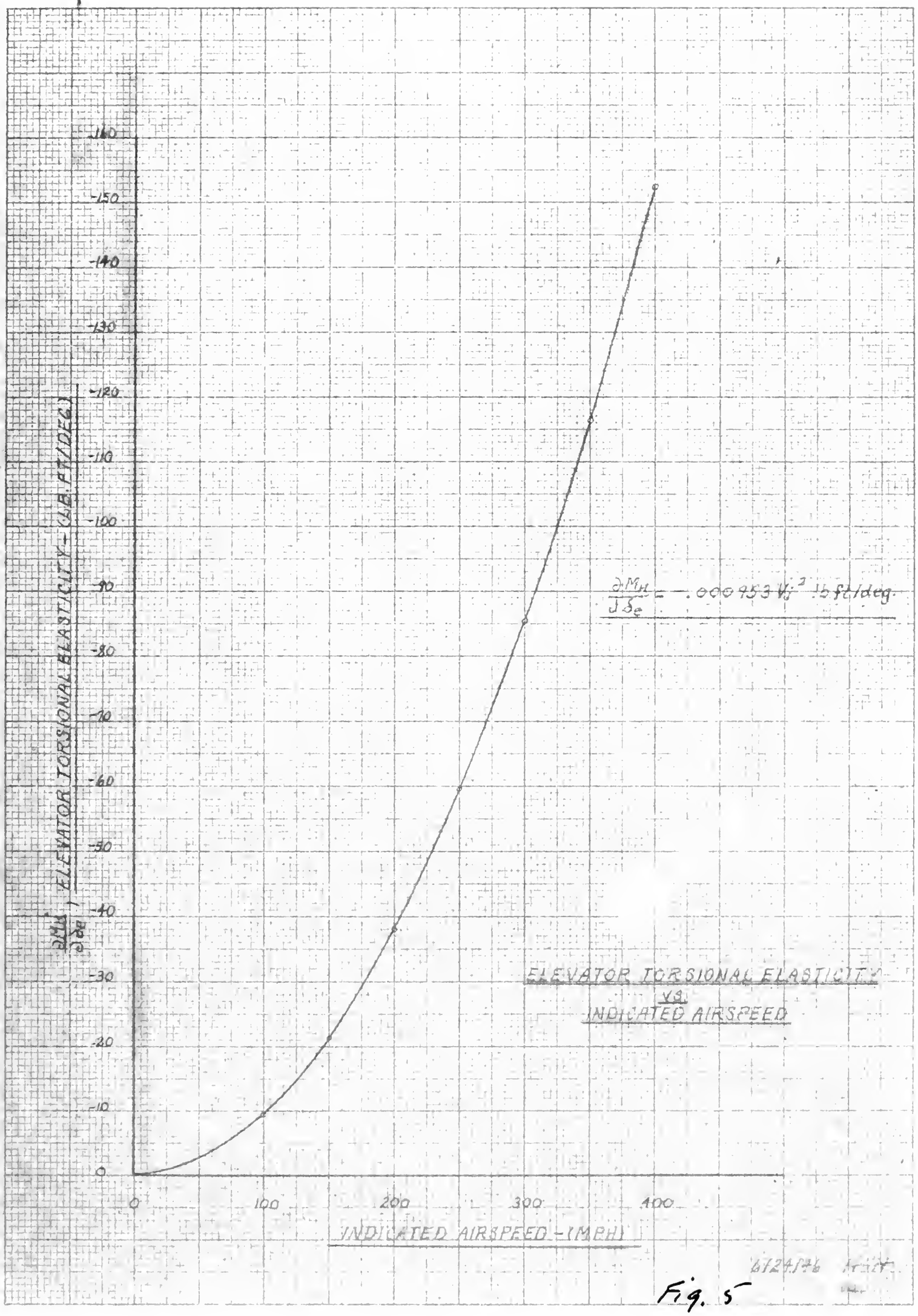
$\frac{\partial M_H}{\partial \delta_e}$ = ELEVATOR TORSIONAL ELASTICITY - (LB. FT./DEG.)
-160
-150
-140
-130
-120
-110
-100
-90
-80
-70
-60
-50
-40
-30
-20
-10
0
0
100
200
300
400
INDICATED AIRSPEED - (MPH)
$\frac{\partial M_H}{\partial \delta_e} = -.000453\, V_i^2$ lb ft/deg.
ELEVATOR TORSIONAL ELASTICITY
vs.
INDICATED AIRSPEED

Fig. 5

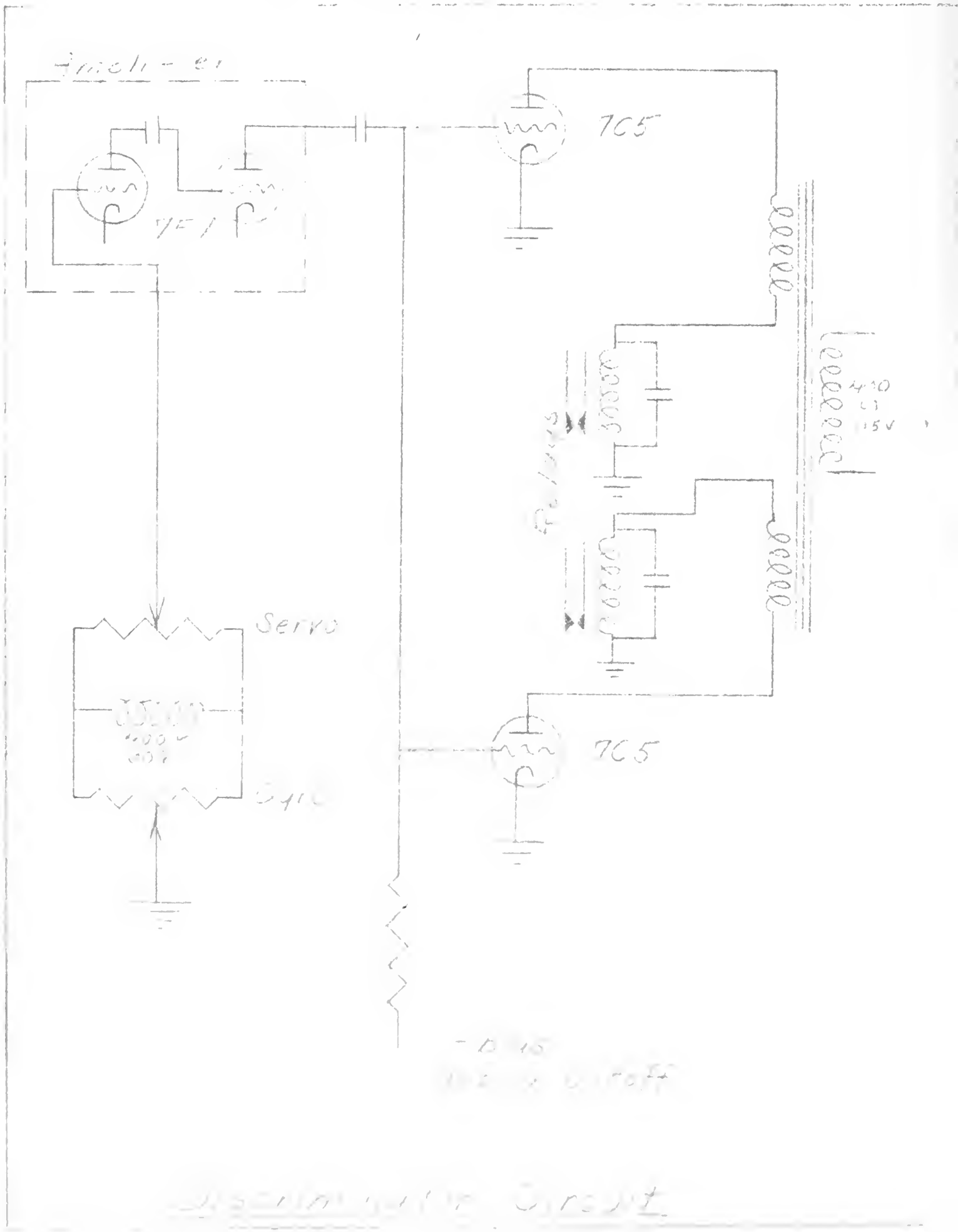

Fig. 6

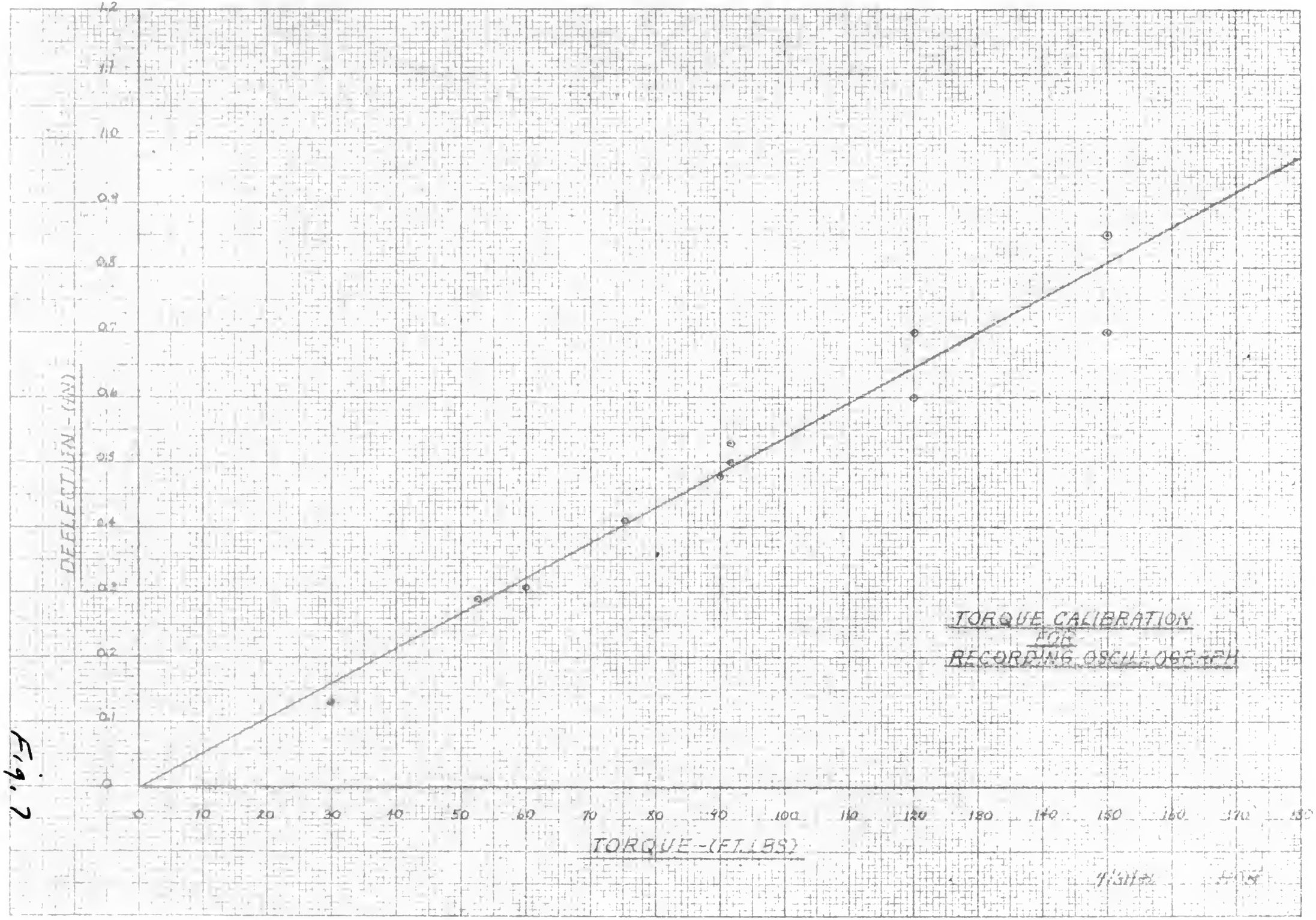
DEFLECTION - (IN)
TORQUE - (FT LBS)
TORQUE CALIBRATION
FOR
RECORDING OSCILLOSCOPE

Fig. 7

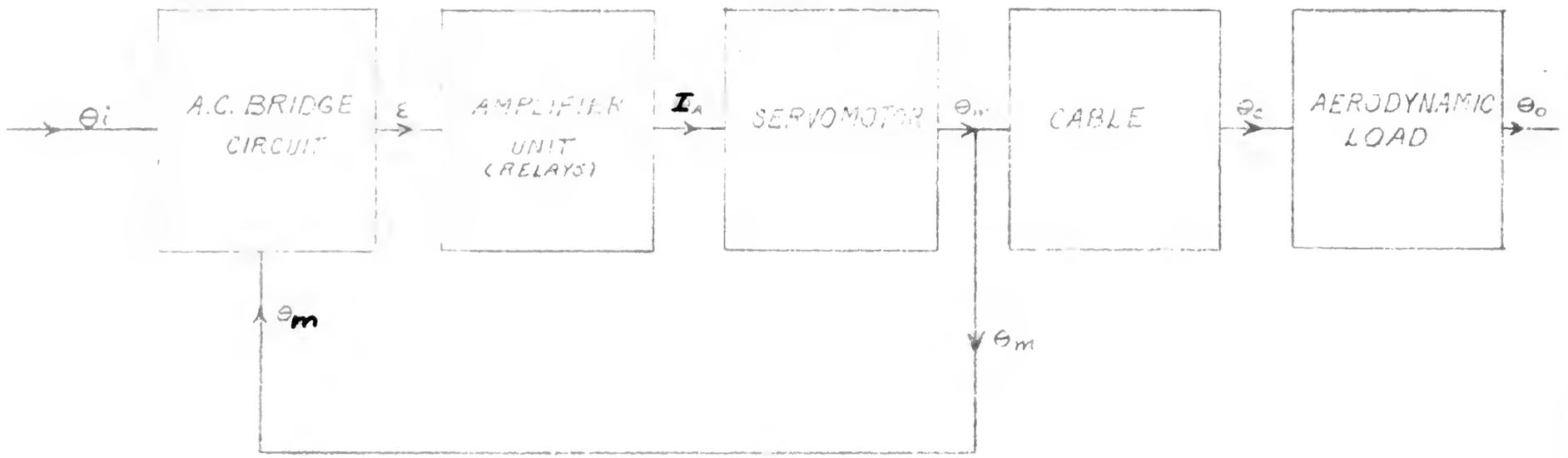

θ_i = ANGULAR POSITION OF FLIGHT GYRO POTENTIOMETER WIPER

θ_o = " " " ELEVATOR

$\varepsilon = \theta_i - \theta_{mi}$

θ_m = ANGULAR POSITION OF CABLE DRUM WIPER

FIG. 13 AUTOPILOT AS A SER. MECHANISM

Fig. 8

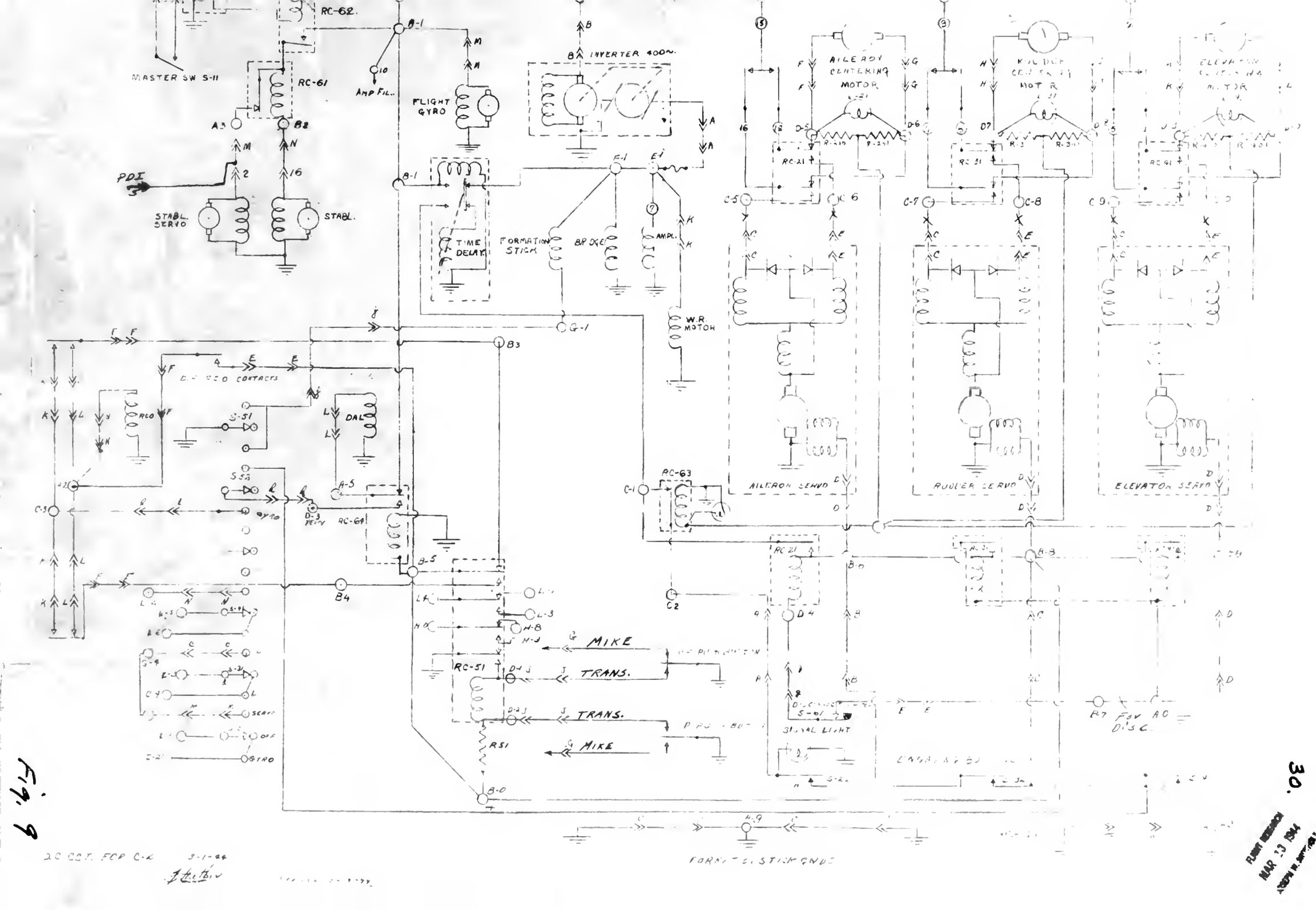
RC-62.
MASTER SW S-11
RC-61
AMP FIL.
FLIGHT GYRO
INVERTER 400 CY.
AILERON CENTERING MOTOR
RUDDER CENTERING MOTOR
ELEVATOR CENTERING MOTOR
PDI
STABL SERVO
STABL.
TIME DELAY
FORMATION STICK
BP DXER
AMPL.
W.R. MOTOR
RC-21
RC-31
RC-41
AILERON SERVO
RUDDER SERVO
ELEVATOR SERVO
RC-63
RC-64
RC-51
RSI
S-51
S-52
DAL
RCO
MIKE
TRANS.
TRANS.
MIKE
SIGNAL LIGHT
D.C. CCO CONTACTS
FORMATION STICK CNDS
AC CCT. FOR C-2
3-1-44

Fig. 9

30.

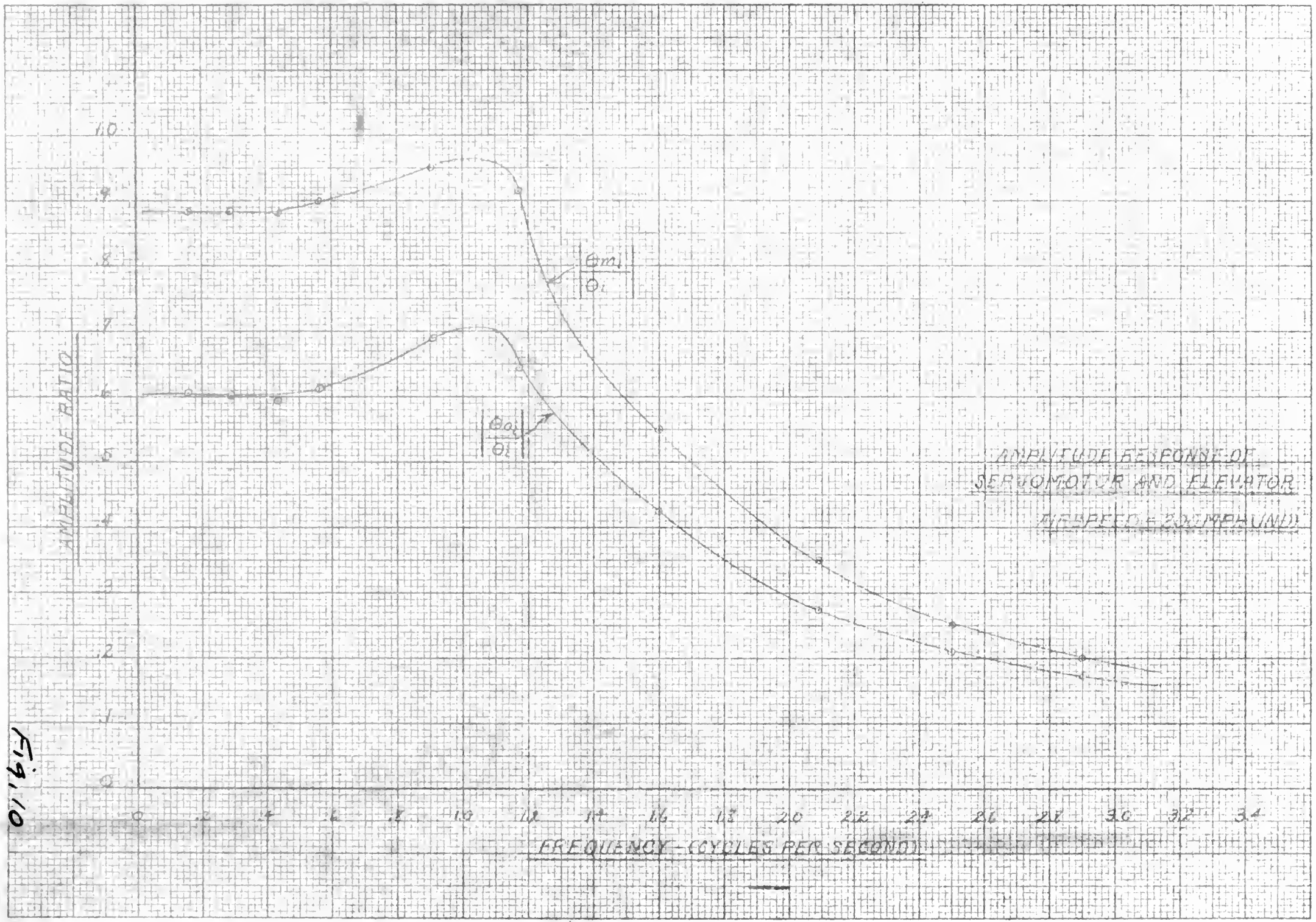

AMPLITUDE RESPONSE OF SERVOMOTOR AND ELEVATOR

AT SPEED = 200 MPH AND

FIG 10

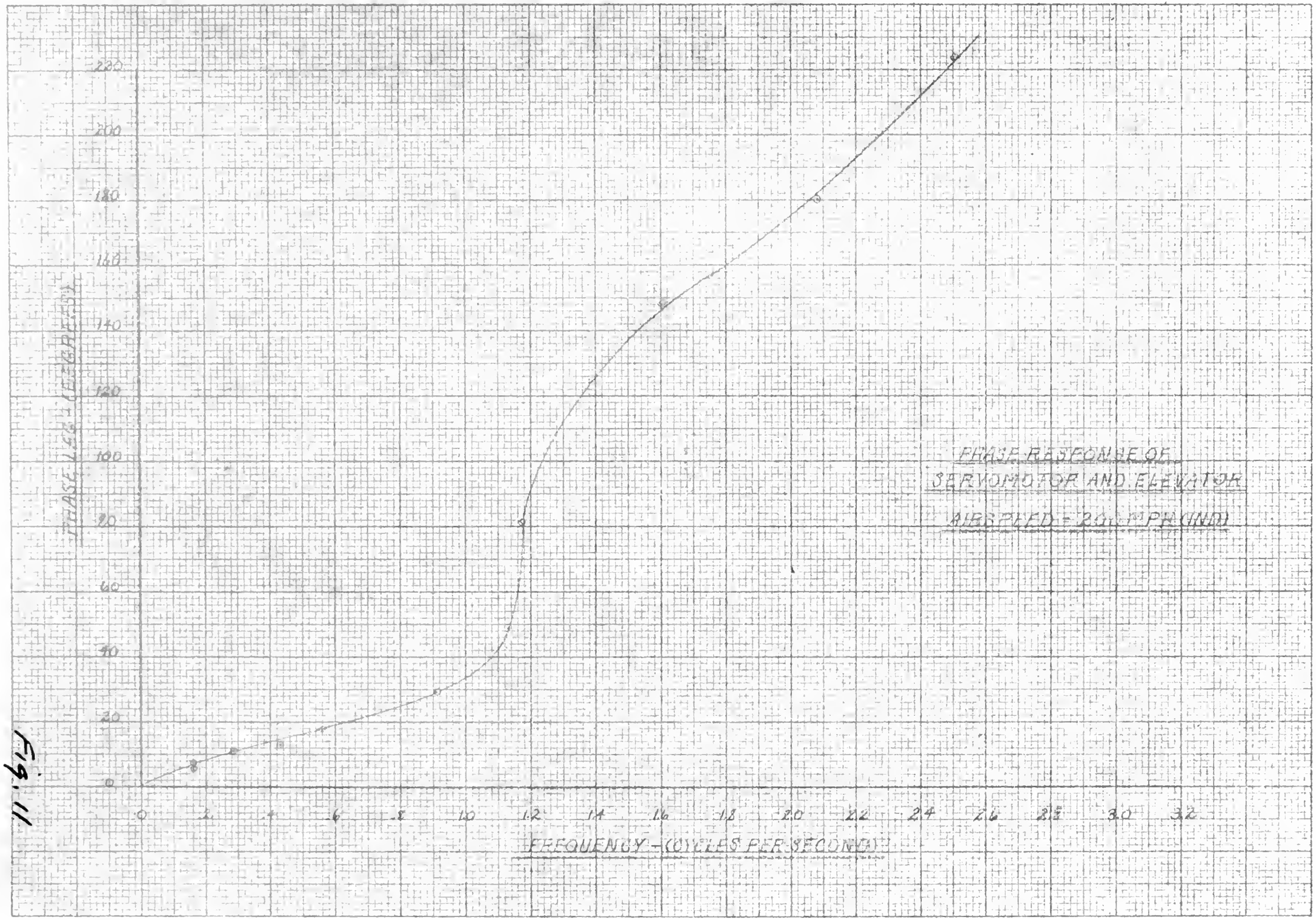
PHASE LAG (DEGREES)
0
20
40
60
80
100
120
140
160
180
200
220
0
.2
.4
.6
.8
1.0
1.2
1.4
1.6
1.8
2.0
2.2
2.4
2.6
2.8
3.0
3.2
FREQUENCY - (CYCLES PER SECOND)
PHASE RESPONSE OF
SERVOMOTOR AND ELEVATOR
AIRSPEED = 200 MPH (IND)

Fig. 11

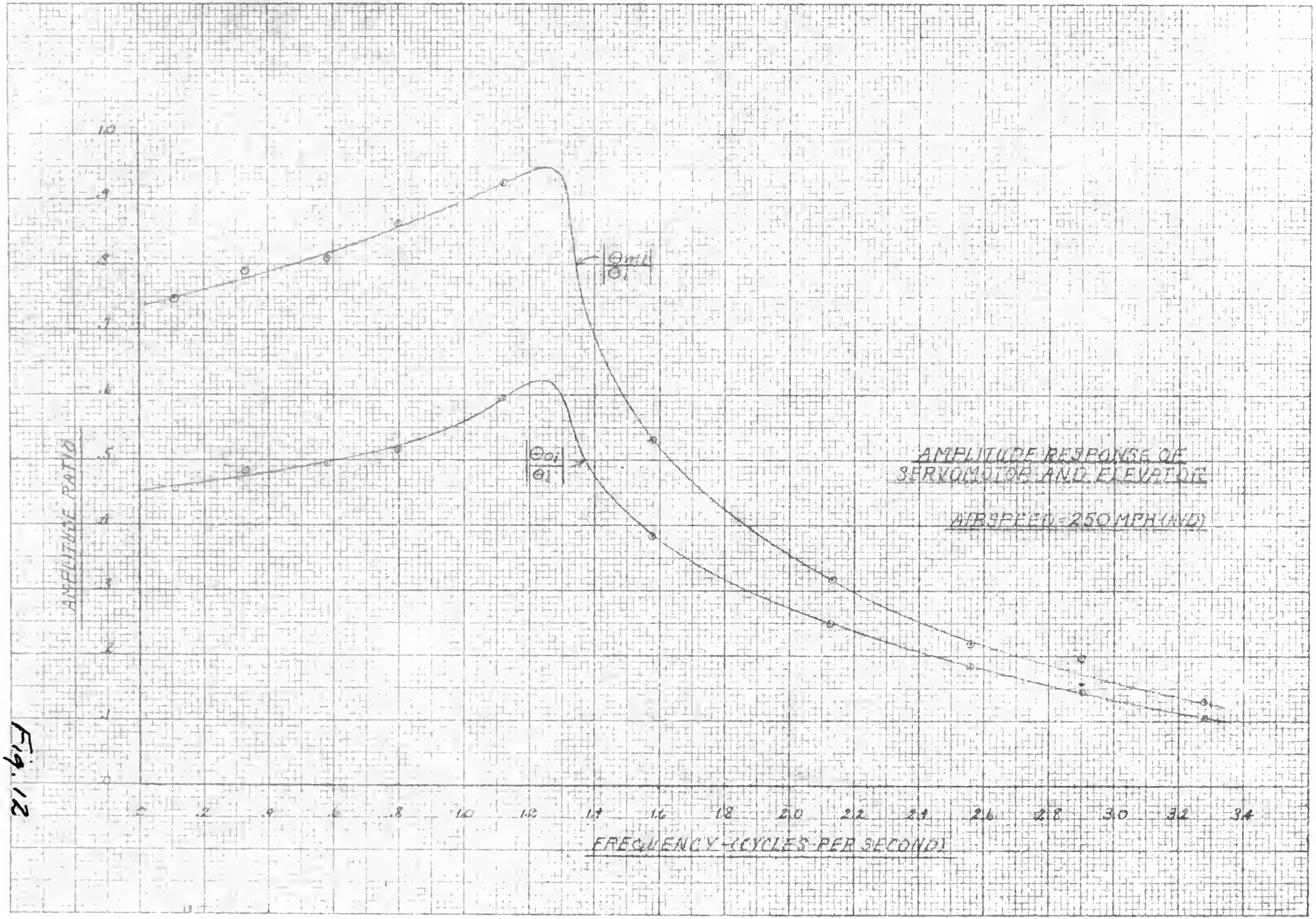
AMPLITUDE RESPONSE OF SERVOMOTOR AND ELEVATOR
AIRSPEED = 250 MPH (A/D)
AMPLITUDE RATIO
FREQUENCY - CYCLES PER SECOND
$\left|\frac{\theta_{act}}{\theta_i}\right|$
$\left|\frac{\theta_{ai}}{\theta_i}\right|$
1.0
.9
.8
.7
.6
.5
.4
.3
.2
.1
0
.2
.4
.6
.8
1.0
1.2
1.4
1.6
1.8
2.0
2.2
2.4
2.6
2.8
3.0
3.2
3.4

Fig. 12

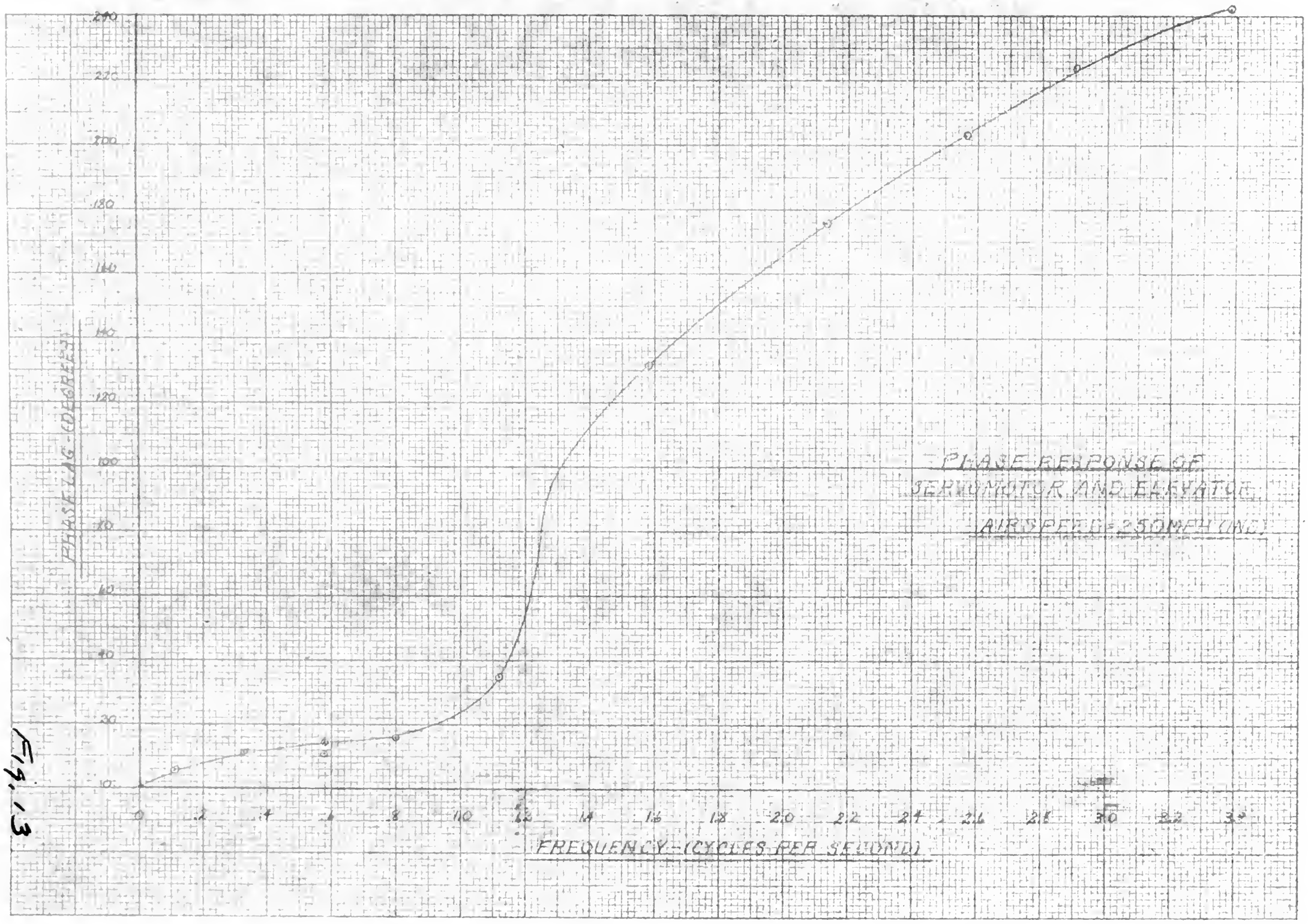
PHASE LAG - (DEGREES)
240
220
200
180
160
140
120
100
80
60
40
20
0
.2
.4
.6
.8
1.0
1.2
1.4
1.6
1.8
2.0
2.2
2.4
2.6
2.8
3.0
3.2
FREQUENCY - (CYCLES PER SECOND)
PHASE RESPONSE OF
SERVOMOTOR AND ELEVATOR
AIRSPEED = 250 MPH (INC.)

Fig. 13

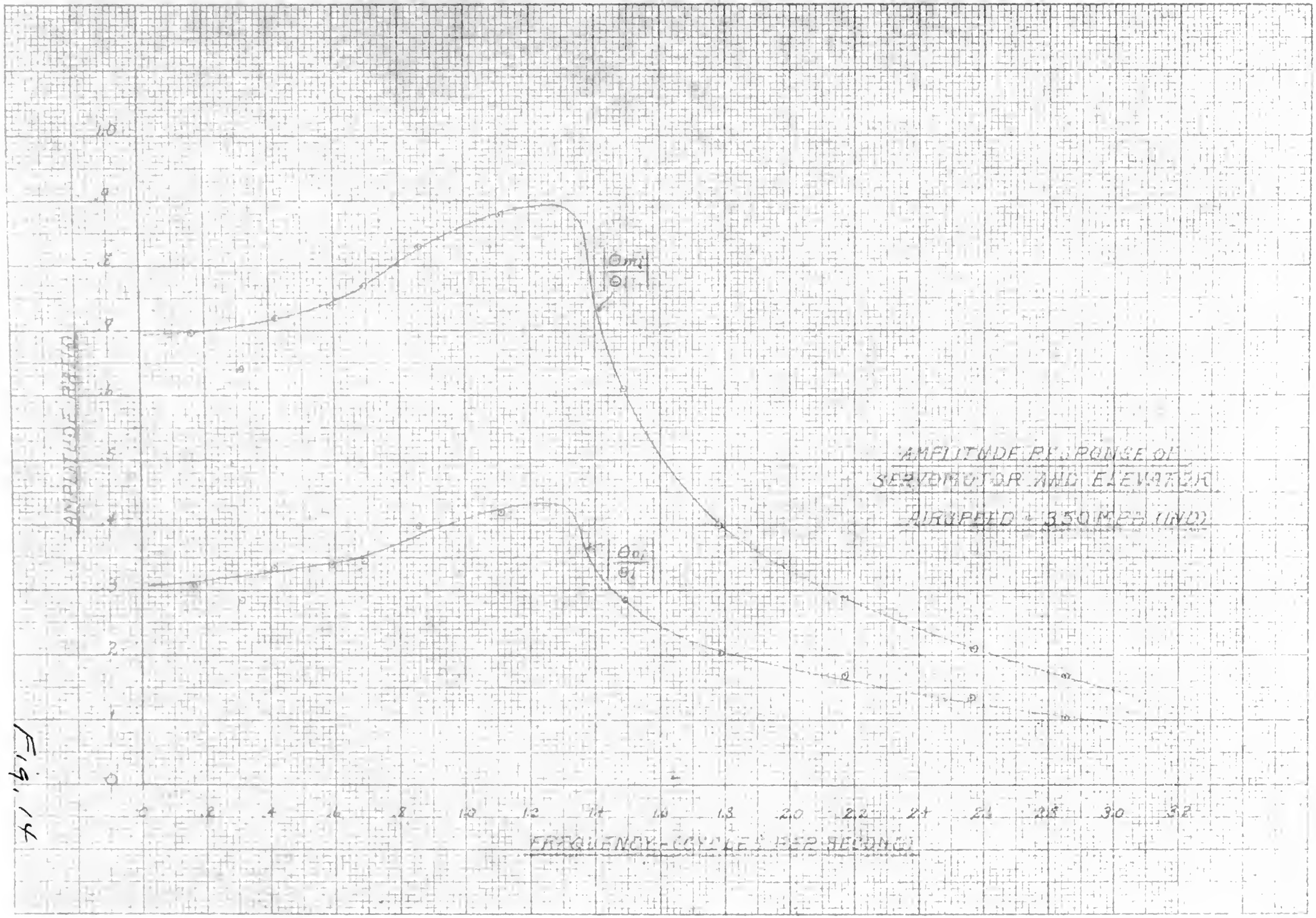

AMPLITUDE RESPONSE OF SERVOMOTOR AND ELEVATOR

AIRSPEED = 350 MPH (IAS)

Fig. 14

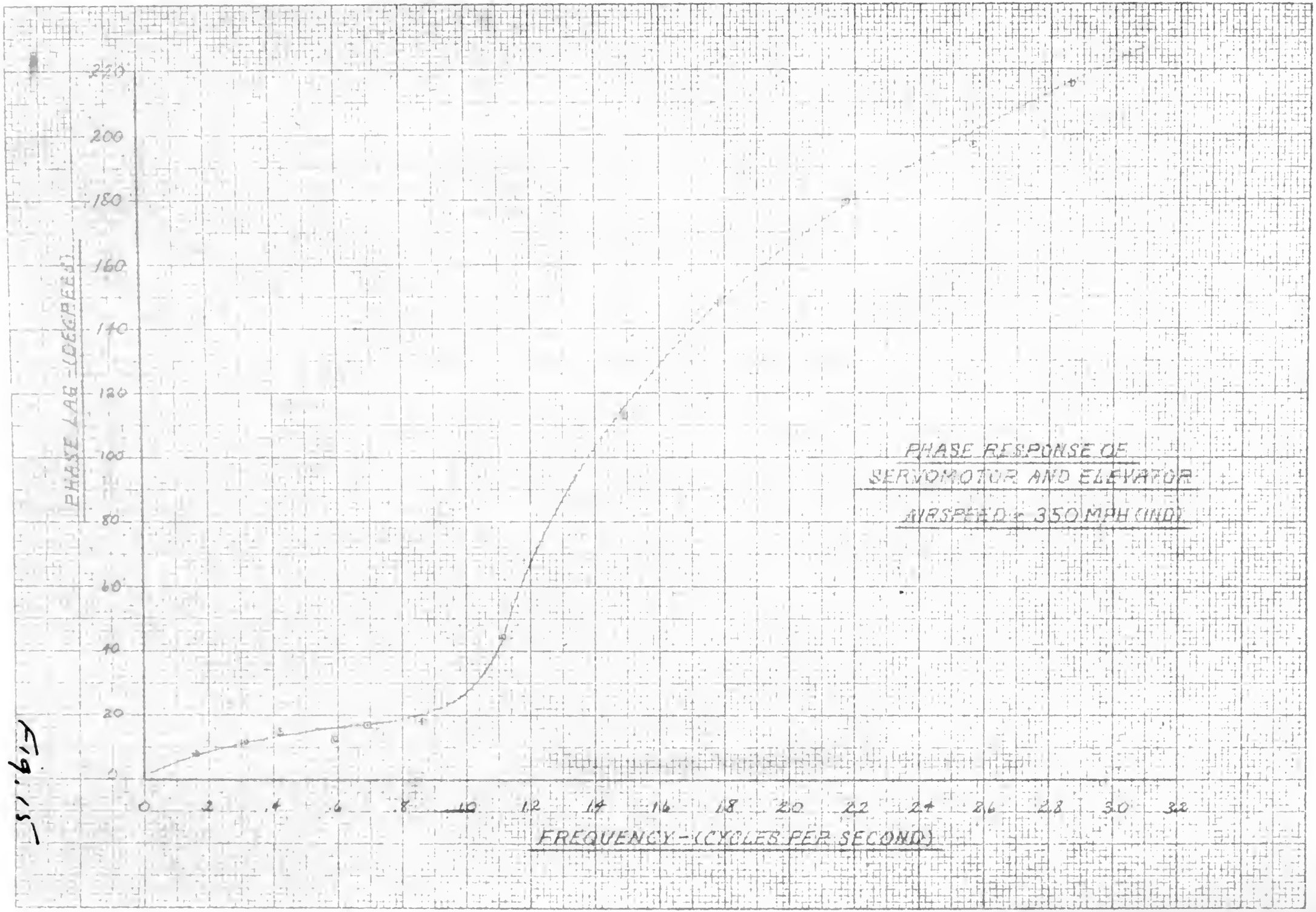
PHASE RESPONSE OF
SERVOMOTOR AND ELEVATOR
AIRSPEED = 350 MPH (IND)
PHASE LAG (DEGREES)
FREQUENCY - (CYCLES PER SECOND)
0
20
40
60
80
100
120
140
160
180
200
220
0
.2
.4
.6
.8
1.0
1.2
1.4
1.6
1.8
2.0
2.2
2.4
2.6
2.8
3.0
3.2

Fig. 17

$\left|\frac{\Theta_o}{\Theta_i}\right|_i(j\omega)$, $\left|\frac{\Theta_m}{\Theta_i}\right|_i(j\omega)$

200 m.p.h.

Frequency - c.p.s.

Reals

$\frac{\Theta_m}{\Theta_i}$

$\frac{\Theta_o}{\Theta_i}$

Fig. 16

MASSACHUSETTS INSTITUTE OF TECHNOLOGY SERVOMECHANISMS LABORATORY D.I.G. NO. _____	DR. B- _____

$\left|\frac{\Theta_o}{\Theta_i}\right|_i(j\omega)$, $\left|\frac{\Theta_m}{\Theta_i}\right|_i(j\omega)$

250 m.p.h.

Frequency - c.p.s.

Reals

$\frac{\Theta_m}{\Theta_i}$

$\frac{\Theta_o}{\Theta_i}$

Fig. 17

MASSACHUSETTS INSTITUTE OF TECHNOLOGY SERVOMECHANISMS LABORATORY D.I.C. NO. _____	DR. B- _____

$\frac{\Theta_o}{\Theta_i}\Big|_i(j\omega)$, $\frac{\Theta_m}{\Theta_i}\Big|_i(j\omega)$

350 m.p.h.

Frequency - c.p.s.

o Reals

$\frac{\Theta_m}{\Theta_i}$

$\frac{\Theta_o}{\Theta_i}$

Fig. 18

MASSACHUSETTS INSTITUTE OF TECHNOLOGY	DR.
SERVOMECHANISMS LABORATORY	B-
D.I.C. NO.	

$\left.\frac{\Theta_m}{E_m}\right|_i (j\omega)$

Frequency - c.p.s.

Reals

240 mph

250 mph

200 mph

Fig. 19

MASSACHUSETTS INSTITUTE OF TECHNOLOGY SERVOMECHANISMS LABORATORY D.I.C. NO.	DR. B-

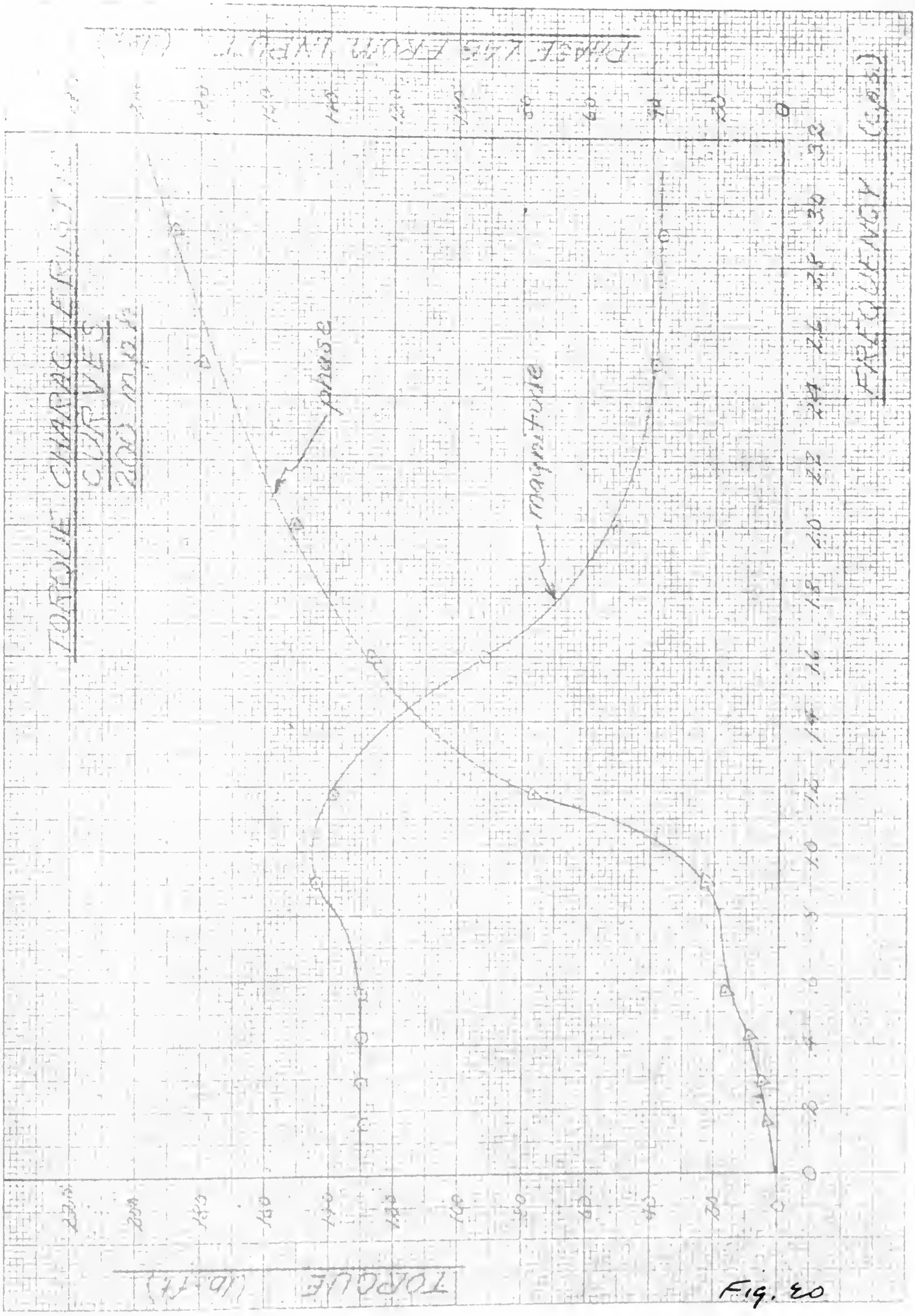
TORQUE CHARACTERISTICS
2000 VOLTS
3 PHASE
Main Armature
PHASE VOLTS FROM LINE TO NEUTRAL (Volts)
ARMATURE CURRENT (Amps)
TORQUE (lb.-ft.)

Fig. 20

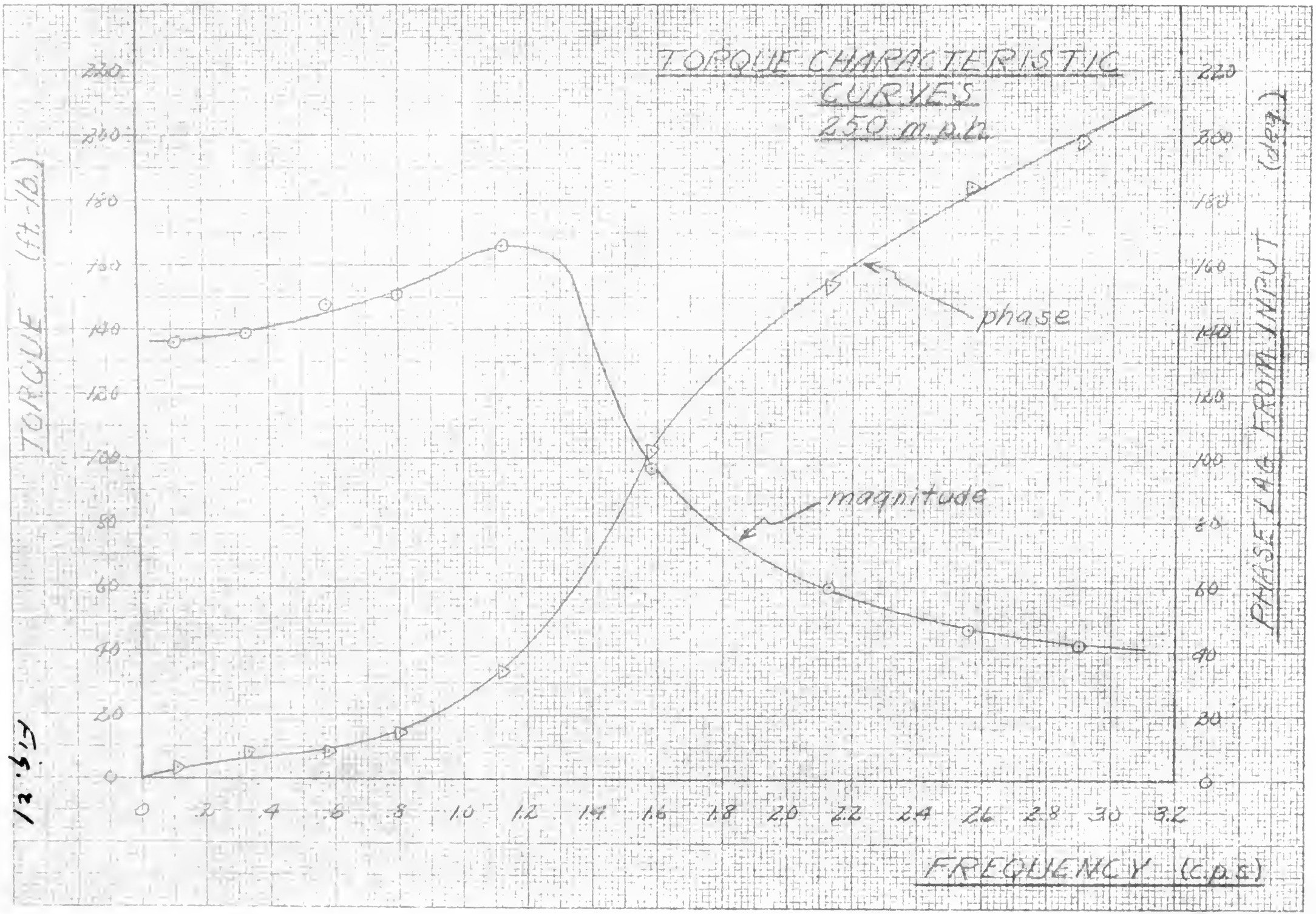
TORQUE CHARACTERISTIC CURVES
250 a.p.h.
TORQUE (ft-lb.)
PHASE LAG FROM INPUT (deg.)
FREQUENCY (c.p.s.)
phase
magnitude
220
200
180
160
140
120
100
80
60
40
20
0
.2
.4
.6
.8
1.0
1.2
1.4
1.6
1.8
2.0
2.2
2.4
2.6
2.8
3.0
3.2
13.5.17

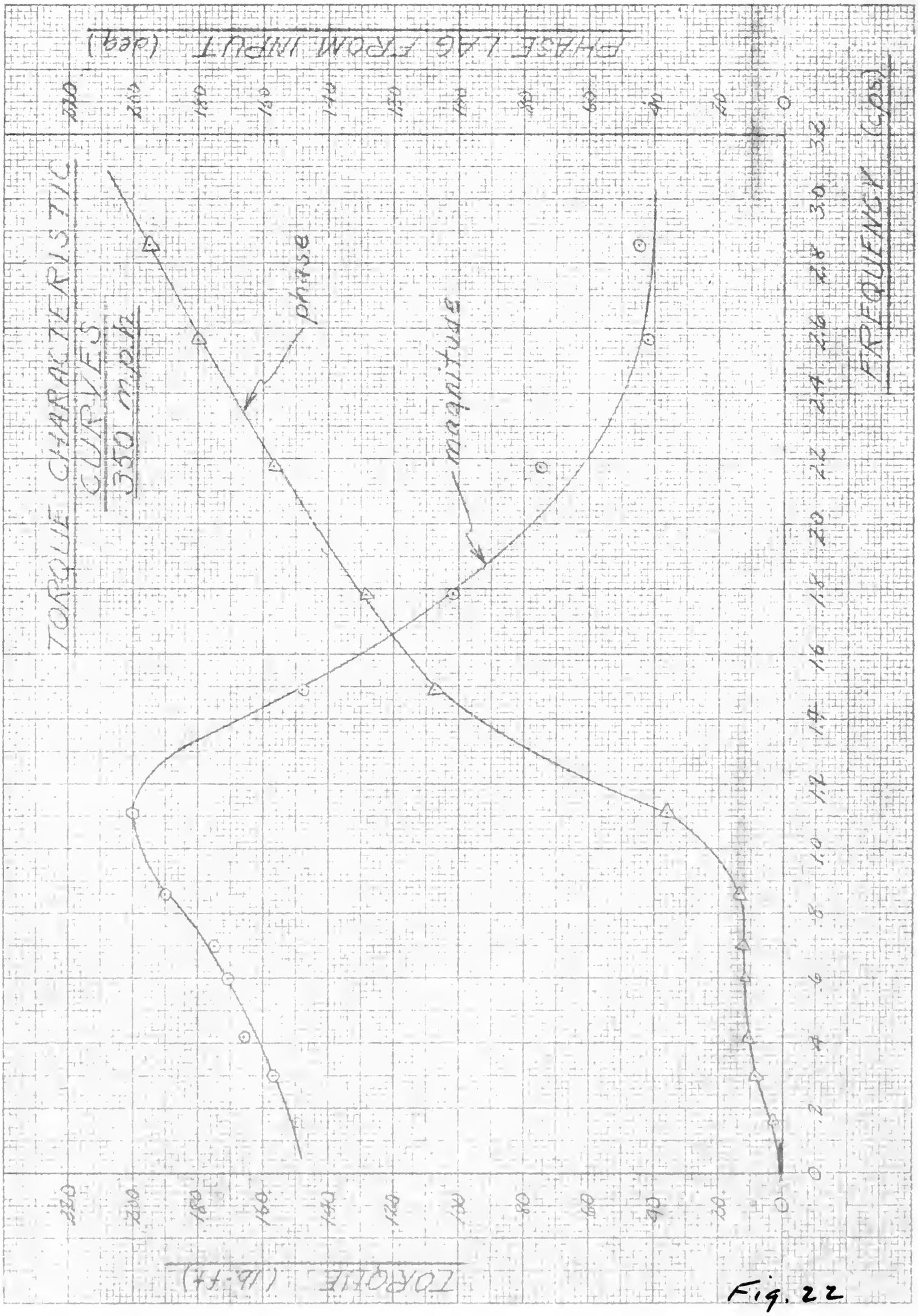
TORQUE CHARACTERISTIC CURVES
350 mm/s
phase
magnitude
PHASE LAG FROM INPUT (deg)
FREQUENCY (cps)
TORQUE (lb-ft)

Fig. 22

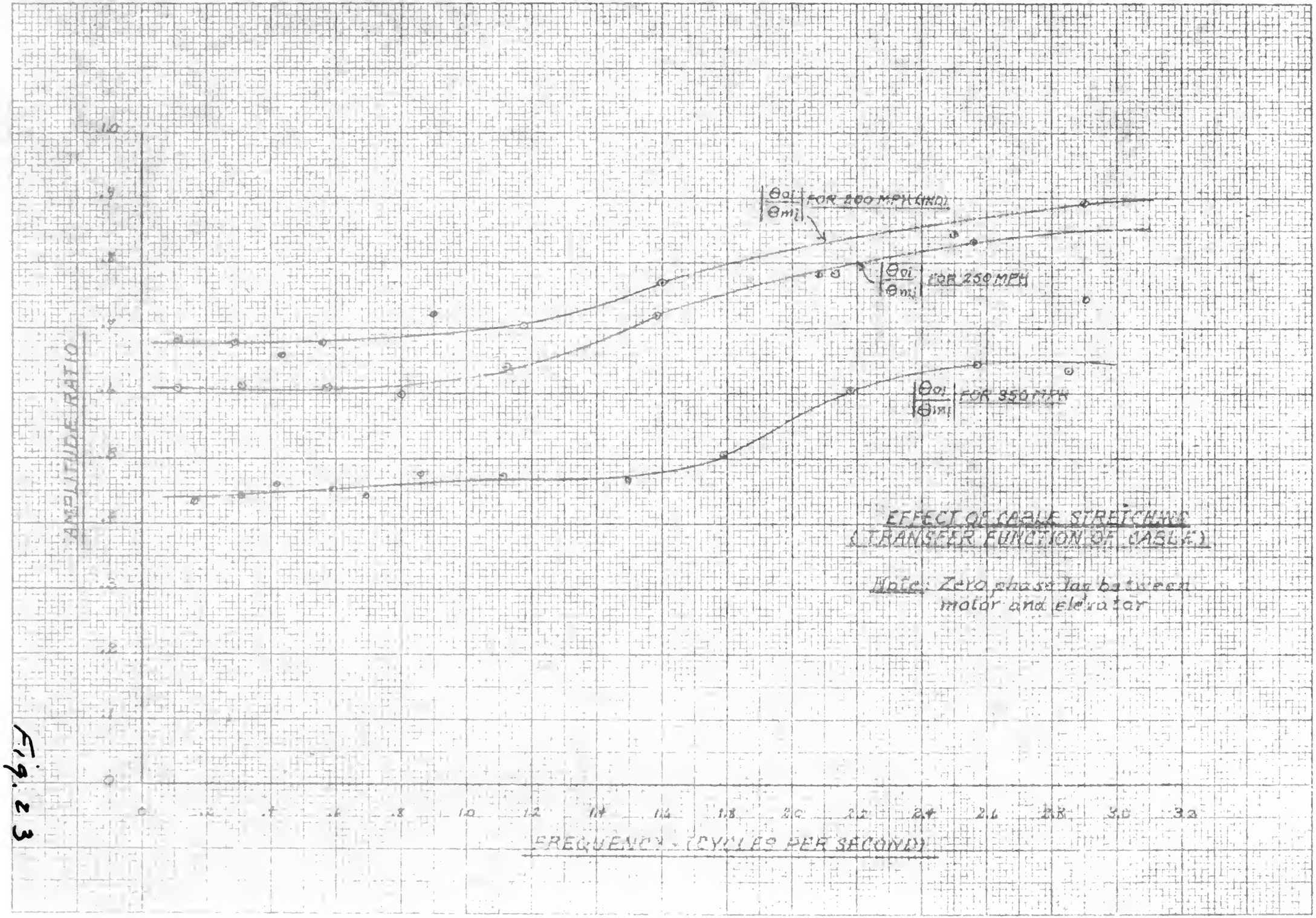
AMPLITUDE RATIO
1.0
.9
.8
.7
.6
.5
.4
.3
.2
.1
0
.2
.4
.6
.8
1.0
1.2
1.4
1.6
1.8
2.0
2.2
2.4
2.6
2.8
3.0
3.2
FREQUENCY - (CYCLES PER SECOND)
|θ0i / θmi| FOR 200 MPH (KNO)
|θ0i / θmi| FOR 250 MPH
|θ0i / θmi| FOR 350 MPH
EFFECT OF CABLE STRETCHING
& TRANSFER FUNCTION OF CABLE)
Note: Zero phase lag between
motor and elevator

Fig. 2.3

INPUT WIPER POSITION
CABLE DRUM POSITION
MOTOR RELAY CLOSURE
ELEVATOR POSITION
ERROR VOLTAGE INDICATION
TORQUE
SAMPLE OSCILLOSCOPE RECORD

Fig. 24

TABLE I

DATA FOR AIRSPEED = 200 MPH (IND)

INPUT	MOTOR OUTPUT (Θ_m)		ELEVATOR ANGLE (Θ_o)		OUTPUT TORQUE (H_o)	
FREQUENCY	MAGNITUDE	+lead −lag PHASE	MAGNITUDE	+lead −lag PHASE	MAGNITUDE	+lead −lag PHASE
Cycles/second	degrees	degrees	degrees	degrees	degrees	degrees
0.161	13.28	− 5.22	2.17	− 7.54	129	− 3.50
0.286	13.28	− 11.32	2.10	− 11.32	130	− 5.10
0.426	13.20	−13.05	2.09	− 13.05	130	− 9.20
0.560	13.50	− 18.15	2.14	−18.15	130	− 16.40
0.905	14.25	− 29.30	2.42	− 29.30	144	− 22.80
1.175	13.72	− 80.60	2.26	− 80.60	139	− 76.30
1.600	8.25	− 138.20	1.49	− 144.00	92	− 127.00
2.085	5.25	− 180.00	0.95	− 180.00	51	− 151.00
2.500	3.75	− 204.50	0.74	− 204.50	39	− 180.00
2.900	3.00	− 224.50	0.63	− 224.50	37	− 188.00

INPUT AMPLITUDE = 7.5 DEGREES

TABLE II

ORIGINAL DATA REFERRED TO INPUT WIPER. AIRSPEED = 200MPH

INPUT	Θ_{mi} referred to input Θ_{mi}		Θ_o referred to input Θ_{oi}		Error of Motor at input ε_{mi}	
FREQUENCY	MAGNITUDE	+ lead − lag PHASE	MAGNITUDE	+ lead − lag PHASE	MAGNITUDE	+ lead − lag PHASE
Cycles / Second	degrees	degrees	degrees	degrees	degrees	degrees
0.161	6.64	− 5.22	4.52	− 7.54	1.05	+ 39.00
0.286	6.64	− 11.32	4.49	− 11.32	1.62	+ 54.80
0.426	6.60	− 13.05	4.44	− 13.05	1.80	+ 55.70
0.560	6.75	− 18.15	4.58	− 18.15	2.35	+ 63.40
0.905	7.12	− 29.30	5.16	− 29.30	3.75	+ 71.00
1.175	6.86	− 50.00	4.84	− 80.60	9.30	+ 47.00
1.600	4.12	− 138.20	3.18	− 144.00	10.90	+ 14.80
2.065	2.62	− 180.00	2.04	− 180.00	10.12	0
2.500	1.87	− 204.50	1.58	− 204.50	9.20	− 5.00
2.700	1.50	− 224.50	1.34	− 224.50	8.60	− 7.00

TABLE III

RESULTS FOR AIRSPEED = 200 MPH

INPUT	$\frac{\Theta_{ai}}{\Sigma_{mi}}$ RATIO		$\frac{\Theta_{ai}}{\Theta_i}$ RATIO		$\frac{\Theta_{mi}}{\Theta_i}$ RATIO		$\frac{\Theta_{ai}}{\Theta_{mi}}$ RATIO	
FREQUENCY	MAGNITUDE	+ lead − lag PHASE	MAGNITUDE	+ lead − lag PHASE	MAGNITUDE	+ lead − lag PHASE	MAGNITUDE	+ lead − lag PHASE
Cycles/Second	—	degrees	—	degrees	—	degrees	—	degrees
0.161	6.32	− 4.22	0.60	− 7.54	0.88	− 5.22	0.68	− 2.32
0.296	4.10	−66.12	0.60	− 11.32	0.88	− 11.32	0.68	0
0.426	3.67	− 68.15	0.54	−13.05	0.88	−13.05	0.66	0
0.560	2.87	−81.55	0.61	−18.15	0.90	−18.15	0.68	0
0.905	1.90	−100.30	0.69	−21.30	0.95	−29.30	0.72	0
1.175	0.74	−127.60	0.64	− 80.60	0.91	−90.62	0.70	0
1.600	0.38	−153.00	0.42	−144.00	0.55	−138.20	0.77	− 5.84
2.035	0.26	−180.00	0.27	−180.00	0.35	−180.00	0.78	0
2.500	0.20	−199.50	0.21	−204.50	0.25	−204.50	0.84	0
2.900	0.17	−217.50	0.18	−234.50	0.20	−224.50	0.90	0

TABLE IV

DATA FOR SPEED = 250 MPH (IND)

INPUT FREQUENCY (f)	MOTOR OUTPUT		FEEDBACK (Hf)		OUTPUT TORQUE (Ho)	
	MAGNITUDE	PHASE (Ref. to Ia)	MAGNITUDE	PHASE (Ref. to Ia)	MAGNITUDE	PHASE (Ref. to Ia)
					FT. LBS	Degrees
[illegible]	[illegible]	[illegible]	[illegible]	- 5.52	136	- 3.54
[illegible]	[illegible]	[illegible]	[illegible]	- 6.04	149	0
[illegible]	[illegible]	- 11.85	[illegible]	- 11.85	139	- 8.30
[illegible]	[illegible]	- 15.62	[illegible]	- 16.40	148	- 8.34
[illegible]	[illegible]	- 17.40	[illegible]	[illegible]	151	- 14.40
[illegible]	[illegible]	[illegible]	[illegible]	[illegible]	166	- 33.80
[illegible]	[illegible]	[illegible]	[illegible]	- 131.50	97	- 103.00
[illegible]	[illegible]	[illegible]	[illegible]	[illegible]	60	- 154.00
[illegible]	[illegible]	[illegible]	[illegible]	[illegible]	47	- 184.50
[illegible]	[illegible]	[illegible]	[illegible]	[illegible]	42	- 198.50
[illegible]	[illegible]	[illegible]	[illegible]	[illegible]	35	- 206.00

INPUT AMPLITUDE = 0.5 DEGREES

TABLE IV

ORIGINAL DATA REFERRED TO INPUT WIPER ; AIRSPEED = 250 MPH

INPUT	Θ_m referred to input Θ_{mi}		Θ_o referred to input Θ_{oi}		Error of Motor at input ε_{mi}	
FREQUENCY	MAGNITUDE	+ lead − lag PHASE	MAGNITUDE	+ lead − lag PHASE	MAGNITUDE	+ lead − lag PHASE
cycles / second	degrees	degrees	degrees	degrees	degrees	degrees
0.1095	5.62	− 6.30	3.42	− 5.52	2.00	− 17.50
0.105	6.10	− 6.04	4.05	− 6.04	1.55	− 24.00
0.329	5.92	− 11.85	3.63	− 11.85	2.10	− 34.00
0.577	6.07	− 15.60	3.69	− 10.40	2.30	− 44.00
0.800	6.52	− 17.40	3.89	− 15.80	2 35	− 56 50
1.120	6.95	− 36.30	4.45	− 35.40	4.50	− 65 50
1.580	4.02	− 131.50	2.90	− 131.50	10.60	− 16 00
2.130	2.40	− 176.00	1.88	− 168.50	9.90	− 1.00
2.560	1.65	− 203.00	1.38	− 208.00	9 00	+ 4.20
2.900	1.50	− 224.00	1.12	− 224.00	8.60	+ 7.00
3.280	0.98	− 242.00	0.81	− 242.00	8.00	+ 6.00

TABLE VI

RESULTS FOR AIRSPEED = 250 MPH

INPUT	$\frac{\theta_m}{\epsilon_m}$ RATIO		$\frac{\theta_a}{\delta_c}$ RATIO		$\frac{\theta_m}{\delta_c}$ RATIO		$\frac{\theta_a}{\epsilon_m}$ RATIO	
FREQUENCY	MAGNITUDE	+lead −lag PHASE	MAGNITUDE	+lead −lag PHASE	MAGNITUDE	+lead −lag PHASE	MAGNITUDE	+lead −lag PHASE
cycles/second	—	degrees	—	degrees	—	degrees	—	degrees
0.122	2.82	−22.20	0.45	−5.52	0.75	−6.30	0.61	+1.90
0.184	3.13	−30.04	0.50	−6.34	0.81	−8.10	0.66	0
0.307	2.81	−45.80	0.45	−11.65	0.79	−14.55	0.51	0
0.511	2.64	−57.0	0.41	−16.20	0.81	−19.80	0.61	+5.20
0.818	2.27	−74.40	0.38	−19.80	0.81	−23.40	0.60	+1.60
1.120	1.54	−106.20	0.29	−32.40	0.92	−36.00	0.64	+0.72
1.636	1.22	−143.00	0.29	−131.50	0.52	−131.50	0.12	0
2.132	0.24	−177.00	0.25	−168.50	0.32	−172.00	0.16	+7.50
2.660	0.19	176.50	0.18	−208.00	0.22	−212.00	0.93	−5.00
3.140	0.17	−211.00	0.15	−214.00	0.20	−216.00	0.15	0
3.660	0.12	−236.00	0.11	−242.00	0.13	−243.00	0.23	0

TABLE VII

DATA FOR AIRSPEED = 350 MPH

INPUT	MOTOR CUTBACK (Gm)		ELEVATOR ANGLE (Gs)		OUTPUT TORQUE (M.)	
FREQUENCY (Cycles/sec)	MAGNITUDE	PHASE + lead - lag Degrees	MAGNITUDE	PHASE + lead - lag Degrees	MAGNITUDE FT-LB.	PHASE + lead - lag Degrees
0.152	1.046	- 5.27	1.031	- 8.59	158	- 2.80
0.278	1.0	- 1.40	1.000	- 12.60	157	- 8.20
0.416	1.2	- 3	1.05	- 15.00	166	- 10.50
0.595	1.12	- 5.25	1.08	- 12.25	171	- 11.80
0.691	1.25	- 10.25	1.215	- 12.50	175	- 12.50
0.838	1.2	- 12.50	1.195	- 13.50	190	- 13.90
1.110	1.3	- 11.00	1.425	- 47.00	200	- 36.00
1.432	9.15	112.5	1.000	- 112.50	148	- 107.50
1.785	6.30	- 149.25	0.714	- 145.00	102	- 128.50
2.172	4.25	- 150.0	0.619	- 180.00	75	- 156.50
2.565	3.15	- 172.50	0.477	- 178.50	42	- 180.00
2.955	2.55	- 216.00	0.381	- 216.00	45	- 195.00

INPUT AMPLITUDE = 7.5 DEGREES

TABLE VIII

ORIGINAL DATA REFERRED TO INPUT WIPER, AIRSPEED = 350 MPH

INPUT	C_{n_β}		C_{l_β}		Error of $\frac{\dot{\beta}b}{2V}$ at input C_{m_β}	
FREQUENCY	MAGNITUDE	+ lead − lag PHASE	MAGNITUDE	+ lead − lag PHASE	MAGNITUDE	+ lead − lag PHASE
Cycles/Second	Degrees	Degrees	Degrees	Degrees	Degrees	Degrees
0.157	5.25	− 8.59	2.21	− 2.59	2.40	+ 18.80
0.303	4.80	− 12.00	2.14	− 12.00	2.95	+ 14.50
0.416	5.40	− 15.00	2.29	− 15.00	2.65	+ 31.50
0.515	5.53	− 12.65	2.24	− 12.25	2.45	+ 31.00
0.611	5.77	− 17.50	2.50	− 17.55	2.65	+ 41.00
0.755	6.25	− 12.25	2.66	− 14.50	2.55	+ 51.50
1.110	6.04	− 41.00	3.15	− 44.00	5.35	+ 60.00
1.492	4.51	− 112.1	2.14	− 112.70	10.15	+ 64.10
1.755	3.40	− 142.00	1.52	− 142.00	10.15	+ 9.30
2.175	2.62	− 180.00	1.32	− 180.00	9.67	0
2.565	1.57	19.50	.92	− 19.50	8.95	− 3.00
2.650	1.32	− 210.00	.81	− 210.00	8.55	− 5.00

TABLE IX

RESULTS FOR APPLE = 35. GPM

TABLE X

CALIBRATION DATA

INPUT - 7.5 DEGREES ON POTENTIOMETER = 1 INCH ON RECORD

MOTOR - 15 DEGREES ON CABLE DRUM = 1 INCH ON RECORD

OUTPUT - 0.64" MOTION AT 15" RADIUS ON TORQUE ARM = 1.0312 INCH ON RECORD.
2.45 DEGREES OF ELEVATOR MOTION = 1.0312 INCH ON RECORD.
2.38 DEGREES OF ELEVATOR MOTION = 1 INCH ON RECORD

TORQUE - 186 LB. FT. = 1 INCH ON RECORD

SYSTEM ALIGNED
ERROR VOLTAGE = 0

~ SAMPLE CALCULATIONS ~

1. DERIVATION OF TORSIONAL ELASTICITY - $\frac{\partial M_H}{\partial \delta_e}$

From A-26 data:

$C_{H_\delta} = -.009$, $C_{H_\alpha} = -.005$; $C_H = C_{H_\delta}\delta_e + C_{H_\alpha}\alpha$

$$M_H = \frac{C_H S_e C_e V_i^2 (mph)}{391}$$

Then:

$$\frac{\partial M_H}{\partial \delta_e} = \frac{\partial C_H}{\partial \delta_e}\,\frac{S_e C_e V_i^2 (mph)}{391}\ ;\ \text{and}\ \frac{\partial C_H}{\partial \delta_e} = C_{H_\delta} = -.009$$

$$\frac{\partial M_H}{\partial \delta_e} = -\frac{.009\,(22.36)(1.35)\,V_i^2}{391} = -.000953\,V_i^2\ \text{lb ft/deg}$$

2. DERIVATION OF SPRING STIFFNESS COEFFICIENT - K

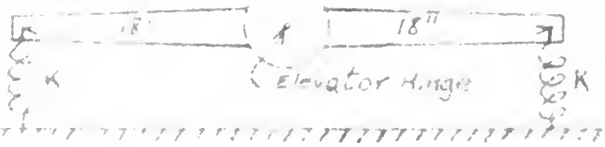

From above: $\frac{\partial M_H}{\partial \delta_e} = -.000953\,V_i^2$ lb ft/deg

$$K = \frac{\text{lb ft}}{\text{deg}} \times \frac{\text{deg}}{\text{rad}} \times \frac{1}{\text{ft}} \times \frac{\text{rad}}{1} = \frac{\text{lb}}{\text{ft}} = \frac{\partial M_H}{\partial \delta_e} \times 57.3 \times \frac{1}{30} \times \frac{1}{18}$$

$$= 1.062\,\frac{\partial M_H}{\partial \delta_e}\ \text{lb/in}$$

3. SIMULATION OF SYSTEM INERTIA - I

From A-26 data:

Elevator inertia about hinge line = 2×620 lb in^2 = 12400

Inertia of Elevator Test Assembly about hinge line = 313 lb in^2

Inertia weights added at 15" each side of hinge = 2 @ 4.5 lb

Added inertia = $2 \times 4.5 \times 15^2$ = 4320 lb in^2

Total Inertia = 7813 + 4320 = 12133 lb in^2

Increase by dynamic response to match natural frequency:

Natural frequency, ω_n = 8.0 cps = 16π rad/sec

$\frac{\partial M_H}{\partial \delta_e}$ at 350 mph = $-.000953 \times 350^2 \times 57.3$ lb in/deg = 30,300 lb in/rad

$$\omega_n = \sqrt{\frac{\partial M_H / \partial \delta_e}{I/g}}\ ;\quad I = \frac{\partial M}{\partial \delta_e} \times g \times \frac{1}{\omega_n^2} = \frac{\text{lb in}}{\text{rad}} \cdot \frac{\text{in}}{\text{sec}^2} \times \frac{\text{sec}^2}{\text{rad}^2} = \text{lb in}^2$$

$$I = \frac{30{,}300 \times 386}{(16\pi)^2} = 12{,}300\ \text{lb in}^2\ \checkmark$$

~SAMPLE CALCULATIONS~

4. DERIVATION OF VISCOUS DAMPING COEFFICIENT - C

From A-26 data:

Hinge Position = .75 ft aft of elevator leading edge

Elevator Chord = 5.43 ft — Tail Chord = 5.43 ft

Elevator Surface Area = 32.6 sq ft — Hinge Position = .405 chord

Wing Chord = 8.14 ft — Half wing chord = 4.07 ft

$$\frac{c_t}{c_w} = \frac{5.43}{8.14} = .668 \qquad \frac{d C_L}{d\alpha} = 5.16 \text{ per rad}$$

From N.A.C.A. Technical Report No 709:

$$C_{H_\delta} = -\frac{\partial C_H}{\partial D_2}\Big|_A + \frac{d C_L}{d\alpha}\left(\frac{\partial C_H}{\partial D_\delta}\right)_B$$

$$\left(\frac{\partial C_H}{\partial D_\delta}\right)_A = .2 \times .668 = .238 \; ; \; \left(\frac{d C_H}{d \delta_e}\right)_B = .12 \times .668 = .0741$$

$$-H_{D_\delta} = 1.238 + 5.16 \times .0741 = 1.595 \text{ per } \frac{d \delta_e}{d S} \text{ (radian, } \tfrac{1}{2} \text{ wing chord)}$$

{ $C_{H D_\delta}$ as found above applies to elevator angle changes with distance along the flight path, S, — to employ the same formula, it must be modified to apply to elevator angle changes with respect to time, S is measured in ½ wing chords. }

$$C_{H_{\dot\delta}} = \frac{1}{\frac{rad}{\frac{1}{2} chord}} \cdot \frac{rad}{sec} = \frac{rad}{\frac{1}{2} chord} \times \frac{ft}{sec} \times \frac{\frac{1}{2} chord}{ft} = .246$$

(V airspeed)

$$C_{H_{D_\delta}} (\text{per rad/sec}) = \frac{H_{D_\delta} \text{ per rad/½ wing chord}}{V, ft/sec \times .246} = \frac{H}{S_e \rho_{1/2} V^2 C_e}$$

Then;

$$\frac{1.595}{.246\, V} = \frac{H}{S_e \rho_{1/2} V^2 C_e} = \frac{H}{(32.6)(.00119)\, V^2}$$

$$C_1 = H \text{ per rad/sec} = 3.633\, V_{(mph)_{true}} \frac{lb\text{-}ft}{rad/sec}$$

$$C_1 = H \text{ per deg/sec} = \frac{.0119}{.0119}\, V_{(mph)_{true}} \frac{lb\text{-}ft}{deg/sec}$$

BIBLIOGRAPHY

1. Draper, C. S. and McKay, W. Instrument Analysis.
2. Hall, A. C. The Analysis and Synthesis of Linear Servomechanisms.
3. A-26 Erection and Maintenance Manual.
4. Overhaul Instructions for Automatic Pilot, Type C1.
5. Den Hartog, J. P. Mechanical Vibrations. McGraw-Hill, 1934.
6. Lin, S. N. Mathematical Study of the Controlled Motion of Airplanes. Sc.D. Thesis, A.E., M.I.T. 1939.
7. Callendar, A., Hartree, D. R., and Porter, A. Time Lag in a Control System. Philosophical Transactions. Royal Society of London, Vol. 235, 1936.
8. Theodorsen, T. General Theory of Aerodynamic Instability and the Mechanism of Flutter. N.A.C.A. Technical Report 496, 1940.
9. Jones, R. T. and Cohen, D. An Analysis of the Stability of an Airplane with Free Controls. N.A.C.A. Technical Report 709, 1941.
10. Mason, C. E. and Philbrick, G. A. Automatic Control in Presence of Process Lag. Paper A.S.M.E. Meeting, Philadelphia, December 1939.

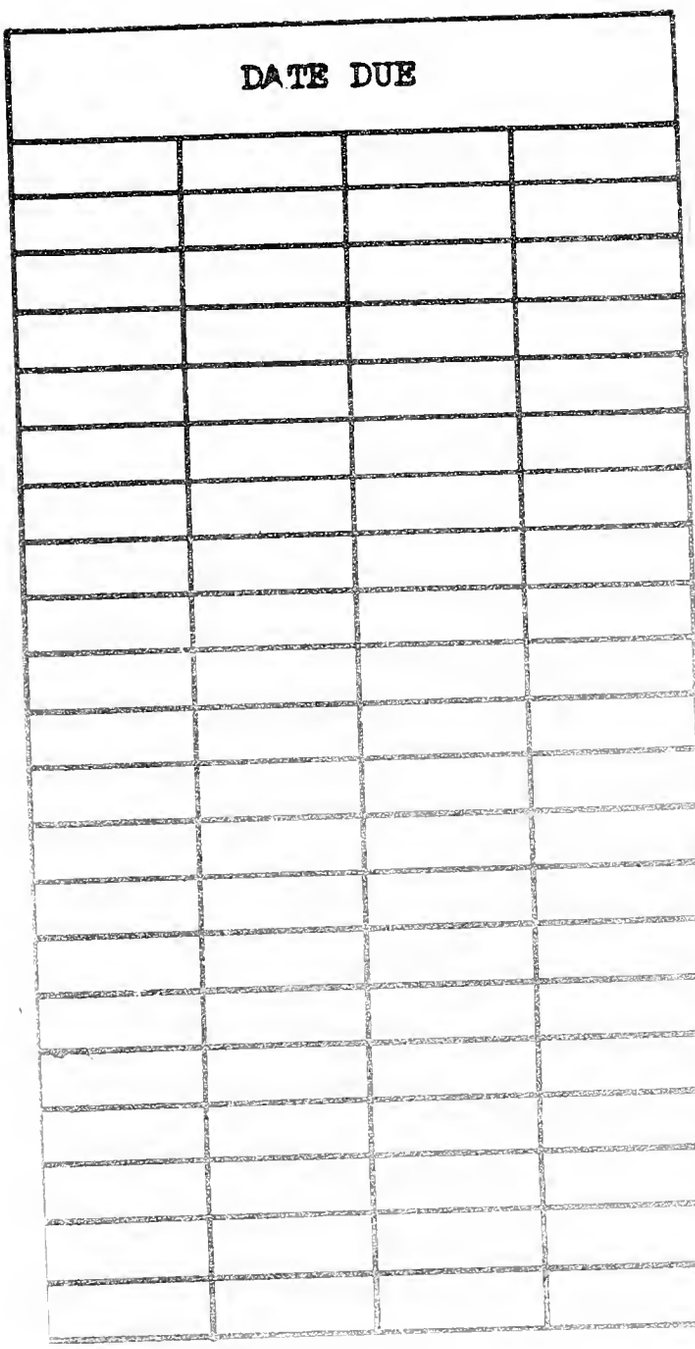
DATE DUE

Thesis 8097
R18 Ralston
Control characteristics of an automatic pilot for aircraft.